RESEARCH MEMORANDUM

for the

Air Materiel Command, Army Air Forces

THE HIGH-SPEED LONGITUDINAL STABILITY AND CONTROL OF THE BELL P-39N-1 AIRPLANE AS CALCULATED FROM PROPELLER-OFF TESTS OF A 0.35-SCALE MODEL

By Robert C. Robinson and Angelo Perone

Ames Aeronautical Laboratory
Moffett Field, Calif.

NATIONAL ADVISORY COMMITTEE
FOR AERONAUTICS

WASHINGTON

JAN 29 1947

NACA RM No.SA6L27

NATIONAL ADVISORY COMMITTEE FOR AERONAUTICS

RESEARCH MEMORANDUM

for the

Air Materiel Command, Army Air Forces

THE HIGH-SPEED LONGITUDINAL STABILITY AND CONTROL OF THE BELL P-39N-1 AIRPLANE AS CALCULATED FROM PROPELLER-OFF TESTS OF A 0.35-SCALE MODEL

By Robert C. Robinson and Angelo Perone

SUMMARY

This report presents the results of tests of a 0.35-scale model of the Bell P-39N-1 airplane. Included are the longitudinal-stability and -control characteristics of the airplane as indicated by tests of the model equipped with each of two different sets of elevators. The results indicate good longitudinal stability and control throughout the speed range encounterable in flight. The variation of estimated stick force with speed was less when the model was equipped with elevators constructed to the theoretical design dimensions than when equipped with elevators as built to scale from measurements of the corresponding parts of the actual airplane. The predicted stick forces required to produce the normal accelerations attainable in flight are within the limits specified by the Army Air Forces.

INTRODUCTION

Tests of a 0.35-scale model of the Bell P-39N-1 airplane have been made in the Ames 16-foot wind tunnel. The purpose of the investigation was to obtain longitudinal-stability and -control data and pressure data for correlation with similar data as measured on the airplane in comprehensive flight tests. To further the success of this correlation, the scale model was designed to reproduce as exactly as possible all details of the specific airplane used in the flight tests. Two different elevators were tested: one scaled down from the actual airplane, and the other built to the theoretical design dimensions.

The general aerodynamic and control characteristics as obtained from the wind-tunnel tests of the model with the propeller off are presented in this report.

DESCRIPTION OF MODEL AND APPARATUS

The 0.35-scale model of the Bell P-39N-1 airplane was designed and built at the Ames Aeronautical Laboratory. In order to assure sufficient strength, and still provide room for a 350-horsepower motor, the fuselage was constructed of a steel frame with a covering of aluminum castings shaped to proper contour. The wing and elevators were constructed of steel spars with mahogany coverings. The lines of the fuselage, vertical tail, and horizontal stabilizer were taken

from the original design dimensions as given by the Bell Aircraft Corporation, while the wing and elevator sections were determined from measurements of the corresponding sections on the airplane used for flight tests. The elevators corresponding to those determined by measurements from the airplane are hereinafter referred to as the "normal elevators," while those having the theoretical sections are referred to as the "theoretical elevators." Elevator hinge moments were measured with an electrical-resistance strain gage.

Various model accessories installed on the model during drag measurements included: two radio masts (fore and aft), a yaw head, two airspeed heads, insulators, and a bomb rack. These items corresponded to the external accessories in place during the flight tests.

The model was mounted in the wind tunnel on the four 5-percent-thick front struts and the 7-percent-thick lower rear strut. The front strut spacing was 76 inches. All struts were unshielded.

A three-view drawing of the model is shown in figure 1. Figure 2(a) shows the model mounted in the tunnel and figure 2(b) shows the model with the various accessories in place.

DIMENSIONAL DATA

The following is a list of the pertinent dimensions of

the model and the airplane:

	0.35-scale model	P-39N-1 airplane
Gross weight, pounds		7629
Wing area, square feet	26.3	213.22
Aspect ratio	5.42	5.42
Span, feet	11.9	34.0
Mean aerodynamic chord, feet	2.352	6.720
Horizontal-tail area, square feet	5.02	40.99
Horizontal-tail span, feet	4.55	13.0
Tail length (c.g. to one-third root chord), feet	5.24	14.95
Elevator area (one), aft of hinge, square feet	0.772	6.30
Elevator span (one), feet	2.14	6.11
Elevator mean-square chord, behind hinge line, square feet	0.125	1.020
Elevator-tab area (each), square feet	0.0702	0.86
Airplane center-of-gravity location, percent M.A.C.		28.5
Distance of center of gravity above M.A.C., feet		0.909
Normal stabilizer incidence relative to thrust axis, degrees	2-1/4	2-1/4

COEFFICIENTS AND SYMBOLS

The data were reduced to the standard NACA coefficients which are based on the model wing area and mean aerodynamic chord. Pitching moments were computed about a center of gravity at 28.5 percent of the mean aerodynamic chord.

The coefficients and symbols used are defined as follows:

C_L	lift coefficient $\left(\frac{\text{lift}}{qS}\right)$
$C_{m_{c.g.}}$	pitching-moment coefficient $\left(\frac{\text{pitching moment}}{qS\ (\text{M.A.C.})}\right)$
C_{h_e}	elevator hinge-moment coefficient $\left(\frac{\text{elevator hinge moment}}{qb_e\ \overline{c_e{}^2}}\right)$
C_D	drag coefficient $\left(\frac{\text{drag}}{qS}\right)$
q	free-stream dynamic pressure $(\frac{1}{2}\rho V^2)$, pounds per square foot
S	wing area, square feet
b_e	effective elevator span, feet
$\overline{c_e{}^2}$	mean square of elevator chord aft of hinge line, square feet
i_t	stabilizer incidence relative to thrust axis, degrees
W	gross weight, pounds
M.A.C.	mean aerodynamic chord, feet
V	velocity, feet per second
V_i	indicated airspeed, miles per hour
V_{mph}	velocity, miles per hour
α_u	uncorrected angle of attack of thrust axis, degrees

α angle of attack of thrust axis corrected for tunnel-wall effects, degrees

α_o angle of attack for zero lift

δ_e elevator deflection, degrees

δ_t elevator trim-tab deflection, degrees

M Mach number $\left(\frac{V}{a}\right)$

a speed of sound, feet per second

h altitude, feet

n indicated acceleration of airplane normal to flight path, expressed in terms of acceleration of gravity

F_s stick force, pounds

REDUCTION OF DATA

The wind-tunnel calibration for dynamic pressure and Mach number was determined from a static-pressure survey of the test section with the model supports in place. Corrections for the constriction due to the model were applied to the Mach number and to the force coefficients. The calibration method and constriction corrections are discussed more fully in reference 1.

Corrections were made for interference of the tunnel wall and the support system. The increments of angle of attack, pitching moment, and drag caused by the tunnel wall were found by the method of reference 2. Tare forces and moments due to the lower struts were evaluated by comparing a run having all four struts in place with one having the

lower struts removed. It was possible to evaluate the effect of the lower struts at negative and small positive lifts only due to limitations on the compressive strength of the struts. The strut compressive strength limit necessitated inverting of the model in order to evaluate the tares due to the pair of struts which enter the wing through the upper surface. The effect of these struts was evaluated only for positive lifts. The rear-strut tares found in tests of a similar model were used.

The stick forces required to maintain the airplane in level unaccelerated flight were calculated from the hinge-moment coefficients corresponding to the elevator angle indicated to be necessary to balance the airplane at the required lift coefficient.

The stick forces required to produce various normal accelerations of the airplane were calculated for the instant that the airplane would be in level flight such as at the bottom of a pull-out from a dive. The elevator deflection and the lift coefficient necessary to produce the desired normal acceleration were found. This lift coefficient was evaluated with consideration of the damping moment of the tail due to the curved flight path of the airplane; that is, the curved flight path causes an effective increase in the incidence of the tail. The elevator deflection and required lift coefficient were used to find the elevator hinge-moment coefficient from which the stick force was then calculated.

RESULTS AND DISCUSSION

Longitudinal Characteristics

The lift, drag, and pitching-moment characteristics of the P-39N-1 model with and without the tail are presented in figures 3 and 4, respectively.

The effect of Mach number on the drag coefficient at various lift coefficients is illustrated in figure 5. Beyond the Mach number of drag divergence the drag increased sharply, the rate of increase becoming greater with increasing lift coefficient. The Mach number of drag divergence obtained from flight tests and presented in reference 3 was 0.04 to 0.05 lower than that obtained in the wind-tunnel tests. Preliminary tests of the model with the propeller indicate that the earlier drag divergence found in the flight tests could be attributed in part to the effects of the propeller. Up to a Mach number of 0.725 the increments in drag due to the tail and to the various accessories (two airspeed heads and a yaw head mounted on booms, two radio masts, a bomb rack, and antenna insulators on the fuselage) were each approximately 0.0025.

The variation with Mach number of the angle of attack for zero lift and of the slope of the lift curve are shown in figure 6. It can be seen that the effect of Mach number on the angle of attack for zero lift is negligible up to a Mach number of 0.8 and that above this value the angle increases

rapidly. The small change in angle of attack for zero lift up to high Mach numbers may be attributed mainly to the symmetrical section of the wing root. The lift-curve slope shows the usual increase with Mach number up to the Mach number of lift divergence, decreasing sharply beyond this point. As can be expected, the variation of lift-curve slope with Mach number depends upon the lift coefficient at which the slopes are measured.

The effects of Mach number on pitching-moment coefficient and lift coefficient are illustrated in figure 7. Both sets of curves reflect the influence of Mach number on the lift-curve slope and the angle of attack for zero lift, the gradual increase of lift coefficient and pitching-moment coefficient up to their Mach numbers of divergence being due largely to the increase of lift-curve slope. Above the Mach numbers of lift and pitching-moment divergence, there is a rapid decrease of lift coefficient and pitching-moment coefficient due to the decrease in airplane lift-curve slope and the increase in the angle of attack for zero lift.

Figure 8 shows that the stabilizer effectiveness $-dC_m/di_t$ increases with Mach number, the value at a Mach number of 0.85 being approximately 33 percent more negative than that at a Mach number of 0.4. This increase of $-dC_m/di_t$, with the decrease of lift-curve slope, at high Mach numbers results in the rapid decrease of pitching-moment coefficient above the Mach number of pitching-moment divergence. Also illustrated in figure 8 is the small effect

of Mach number on the effectiveness $\partial C_m/\partial \delta_e$ of both normal and theoretical elevators. The variation of $\partial C_m/\partial \delta_e$ through the range of angle of attack encountered in high-speed flight was negligible for both elevators. The curves of figure 8 show the theoretical elevator to be about 7 percent more effective than the normal elevator.

The static longitudinal stability of the model is illustrated in figure 9 by the variation with Mach number of the stick-fixed neutral point at three lift coefficients. Here too, the effects of Mach number on airplane lift-curve slope and tail effectiveness may be seen in the greatly increased stability at the higher speeds.

Elevator Control Forces

The variation of pitching-moment coefficient and elevator hinge-moment coefficient with elevator angle for several lift coefficients and Mach numbers is shown in figure 10 for the normal elevator and in figure 11 for the theoretical elevator. Study of these curves reveals that the effect of Mach number on $\partial C_{h_e}/\partial \delta_e$ is small for both elevators and that the value of $\partial C_{h_e}/\partial C_L$ is small and not greatly affected by Mach number within the range of lift coefficients and elevator angles encountered at high speeds. In general, the effects of surface irregularities on the normal elevator were to decrease the elevator effectiveness and the hinge moment.

In figure 12 the variation of elevator trim-tab

effectiveness with Mach number is shown. The tab maintains its effectiveness throughout the Mach number range in which it was tested and is only slightly influenced by moderate variations in elevator angle and lift coefficient.

Figure 13 presents the variation with indicated airspeed of elevator angle and stick force for level flight at three altitudes, with the trim tab neutral. The curves of elevator angle and stick force for sea-level conditions have been extrapolated from the 0.4 Mach number to lower speeds to obtain the trim speed of the airplane. It is apparent that with the theoretical elevator the airplane balances at a lower speed for zero elevator deflection and the stick-fixed stability is in general slightly less than with the normal elevators. The difference in trim speed is equivalent to a small difference in stabilizer incidence, while the decreased stick-fixed stability with the theoretical elevator is evidently due to its greater effectiveness. In spite of the fact that larger deflections of the theoretical elevator were required to balance the model, the normal elevator produced larger stick forces due to the decrease in the hinge moment caused by the deformed surfaces.

Comparison of parts (a), (b), and (c) of figure 13 shows the effects of altitude on the variation of elevator angle and stick force with indicated air speed. In general, the stick-fixed stability increased with altitude, and the stick force increased slightly for a constant indicated airspeed.

At constant Mach number the stick force decreased with increasing altitude.

The calculated stick force required at different altitudes for various normal accelerations in pull-ups is shown in figure 14. At sea level a linear variation of stick force with normal acceleration was calculated for Mach numbers up to about 0.725. The effect of altitude, in general, is to increase the stick-force gradient F_s/n for each particular Mach number. Figure 15 shows that for constant values of normal acceleration, the effect of Mach number on the stick force is negligible until 0.7 Mach number is reached. For Mach numbers above 0.7, the stick force increases more rapidly with speed for the larger values of normal acceleration. In general, at a given Mach number the stick force required to produce a given normal acceleration increases with altitude. The predicted stick forces for normal accelerations encountered in flight are not excessive and are within the limits specified by the Army Air Forces in reference 4.

CONCLUSIONS

The high-speed wind-tunnel tests of the 0.35-scale model of the P-39N-1 indicate the following:

1. The model exhibited an increase in longitudinal stability and a slight diving moment at high Mach numbers, but the available elevator control was sufficient to overcome these tendencies at all flight Mach numbers of the P-39N-1

airplane.

2. The stabilizer effectiveness increased considerably with Mach number, while the elevator effectiveness was practically unchanged.

3. The elevator-tab effectiveness showed no change with Mach number and was little affected by changes in elevator angle and lift coefficient.

4. Comparison of the normal elevators (which were scaled from the actual airplane) with those as constructed from the theoretical design dimensions shows that although smaller deflections of the normal elevators were required for balancing the airplane they produced larger stick forces than did the theoretical elevators.

Ames Aeronautical Laboratory,
National Advisory Committee for Aeronautics,
Moffett Field, Calif.

Robert C. Robinson
Robert C. Robinson,
Aeronautical Engineer.

Angelo Perone
Angelo Perone,
Aeronautical Engineer.

Approved:

Donald H. Wood
Donald H. Wood,
Aeronautical Engineer.

REFERENCES

1. Nissen, James M., Gadeberg, Burnett L., and Hamilton, William T.: Correlation of the Drag Characteristics of a P-51B Airplane Obtained from High-Speed Wind-Tunnel and Flight Tests. NACA ACR No. 4K02, 1945.

2. Silverstein, Abe, and White, James A.: Wind-Tunnel Interference with Particular Reference to Off-Center Positions of the Wing and to the Downwash at the Tail. NACA Rep. No. 547, 1935.

3. Gasich, Welko E., and Clousing, Lawrence A.: Flight Investigation of the Variation of Drag Coefficient with Mach Number for the Bell P-39N-1 Airplane. NACA ACR No. 5D04, 1945.

4. Anon: Stability and Control Requirements for Airplanes. Spec. No. C-1815, Army Air Forces, Aug. 31, 1943.

FIGURE LEGENDS

Figure 1.- Three-view drawing of the .35 scale model of the P-39N-1 airplane.

Figure 2.- The 0.35-scale model of the Bell P-39N-1 airplane as tested in the 16-foot wind tunnel.

Figure 3.- Lift, drag, and pitching-moment characteristics of the P-39N-1 model at several Mach numbers with the tail at the standard setting of 2-1/4° and $\delta_e = 0°$.

Figure 4.- Lift, drag, and pitching-moment characteristics of the P-39N-1 model without a tail at several Mach numbers.

Figure 5.- Variation of drag coefficient with Mach number for the P-39N-1 airplane model.

Figure 6.- Variation of the angle of attack for zero lift and the slope of the lift curve with Mach number. $\delta_e = 0°$; P-39N-1 model.

Figure 7.- The variation of pitching-moment coefficient and lift coefficient with Mach number at several attitudes. $\delta_e = 0°$; P-39N-1 model.

Figure 8.- Variation of stabilizer effectiveness and elevator effectiveness with Mach number for the P-39N-1 model.

Figure 9.- Variation of the stick-fixed center-of-gravity position for neutral stability with Mach number at different values of lift coefficient. P-39N-1 model.

Figure 10.- Variation of pitching-moment and elevator hinge-moment coefficients with elevator angle for constant lift coefficients. Normal elevators; $i_t = 2\text{-}1/4°$; $\delta_t = 0°$; P-39N-1 model. (a) M = 0.4

Figure 10.- Continued. P-39N-1 model. (b) M = 0.55.

Figure 10.- Continued. P-39N-1 model. (c) M = 0.65.

Figure 10.- Continued. P-39N-1 model. (d) M = 0.70

Figure 10.- Continued. P-39N-1 model. (e) M = 0.725

Figure 10.- Continued. P-39N-1 model. (f) M = 0.75

Figure 10.- Continued. P-39N-1 model. (g) M = 0.775

Figure 10.- Continued. P-39N-1 model. (h) M = 0.80.

Figure 10.- Continued. P-39N-1 model. (i) M = 0.825

Figure 10.- Concluded. P-39N-1 model. (j) M = 0.85

Figure 11.- Variation of pitching-moment and elevator hinge-moment coefficients with elevator angle for constant lift coefficients. Theoretical elevators; $i_t = 2\text{-}1/4^\circ$; $\delta_t = 0^\circ$; P-39N-1 model. (a) M = 0.4.

Figure 11.- Continued. P-39N-1 model. (b) M = 0.55.

Figure 11.- Continued. P-39N-1 model. (c) M = 0.65.

Figure 11.- Continued. P-39N-1 model. (d) M = 0.70.

Figure 11.- Continued. P-39N-1 model. (e) M = 0.725.

Figure 11.- Continued. P-39N-1 model. (f) M = 0.75.

Figure 11.- Continued. P-39N-1 model. (g) M = 0.775

Figure 11.- Continued. P-39N-1 model. (h) M = 0.80

Figure 11.- Continued. P-39N-1 model. (i) M = 0.825

Figure 11.- Concluded. P-39N-1 model. (j) M = 0.85

Figure 12.- Variation of elevator trim-tab effectiveness with Mach number at different elevator angles and lift coefficients. P-39N-1 model.

Figure 13.- Variation of elevator angle and stick force with indicated airspeed for balance of the P-39N-1 airplane in level flight. As predicted from tests of a 0.35-scale model. $\delta_t = 0^\circ$; $i_t = 2\text{-}1/4^\circ$. (a) Sea level.

Figure 13.- Continued. P-39N-1 model. (b) h = 15000 feet.

Figure 13.- Concluded. P-39N-1 model. (c) h = 25000 feet.

Figure 14.- Variation of stick force with indicated normal acceleration for various Mach numbers at different altitudes. Normal elevators; $i_t = 2\text{-}1/4^\circ$. P-39N-1 model.

Figure 15.- Variation of stick force with Mach number for constant values of indicated normal acceleration. Normal elevators; $i_t = 2\text{-}1/4^\circ$; P-39N-1 model.

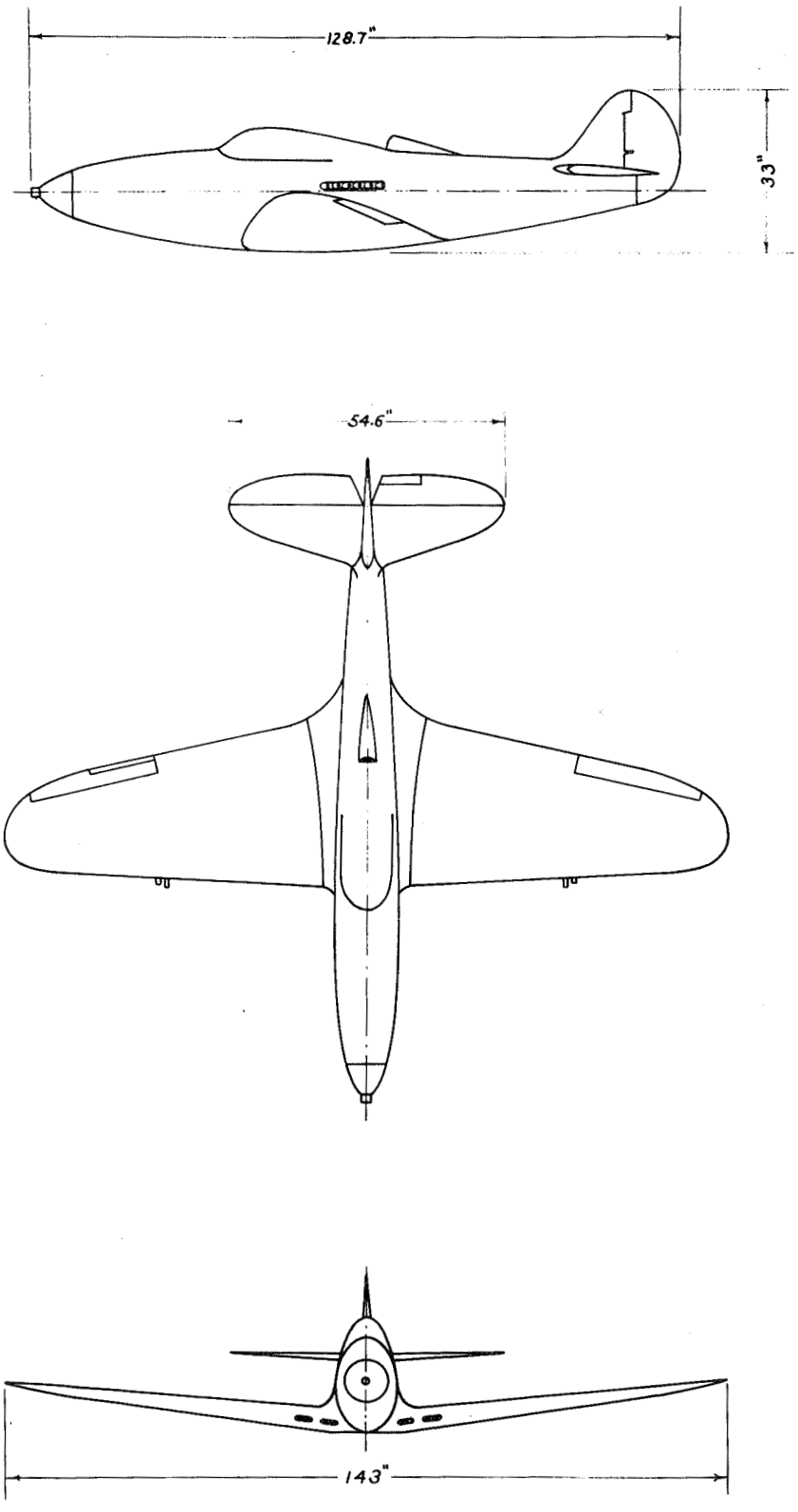

FIGURE 1.- THREE-VIEW DRAWING OF THE .35 SCALE MODEL OF THE P-39N-1 AIRPLANE.

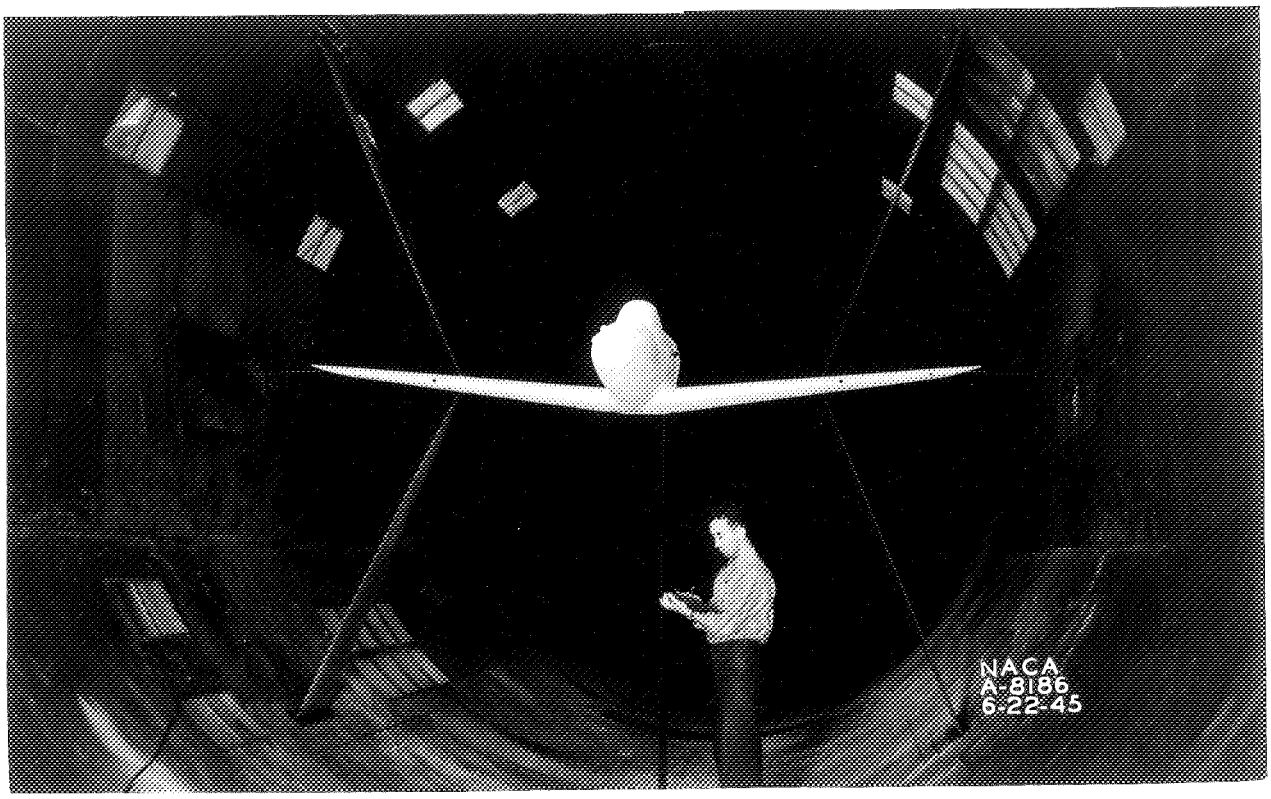

(a) Front view of the P-39N-1 model mounted in the tunnel.

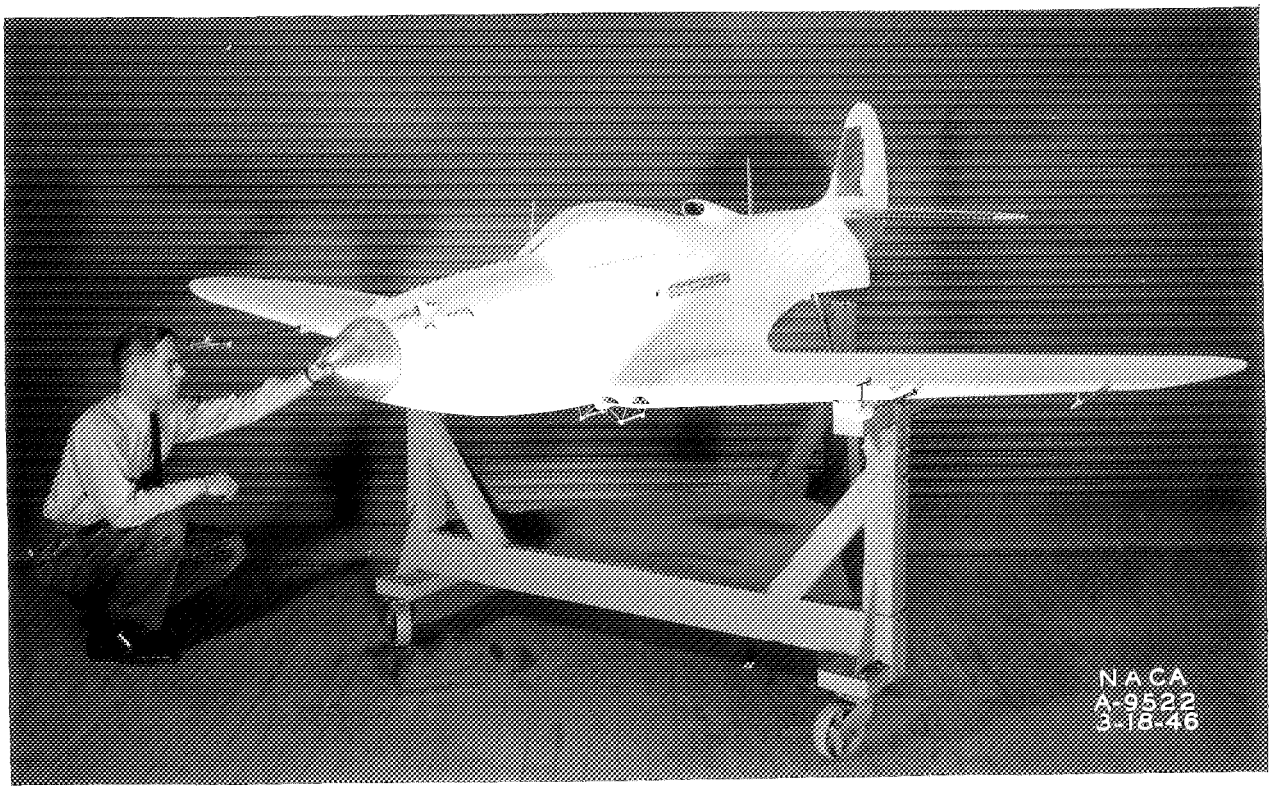

(b) Three-quarter front view of the P-39N-1 model showing accessories in place.

Figure 2.- The 0.35-scale model of the Bell P-39N-1 airplane as tested in the 16-foot wind tunnel.

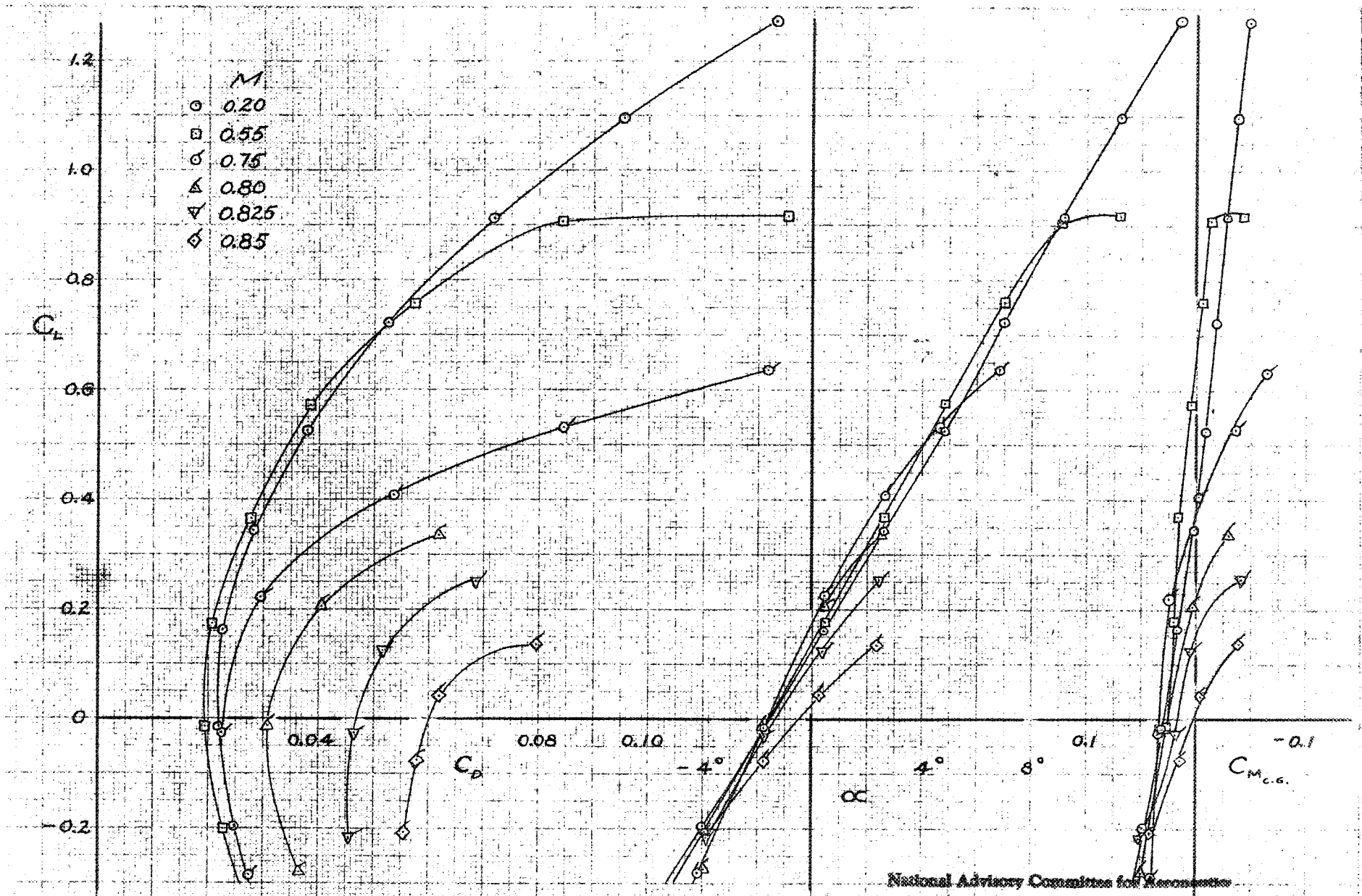

FIGURE 3.— LIFT, DRAG, AND PITCHING-MOMENT CHARACTERISTICS OF THE P-39N-1 MODEL AT SEVERAL MACH NUMBERS WITH THE TAIL AT THE STANDARD SETTING OF 2¼° AND $\delta_e = 0°$

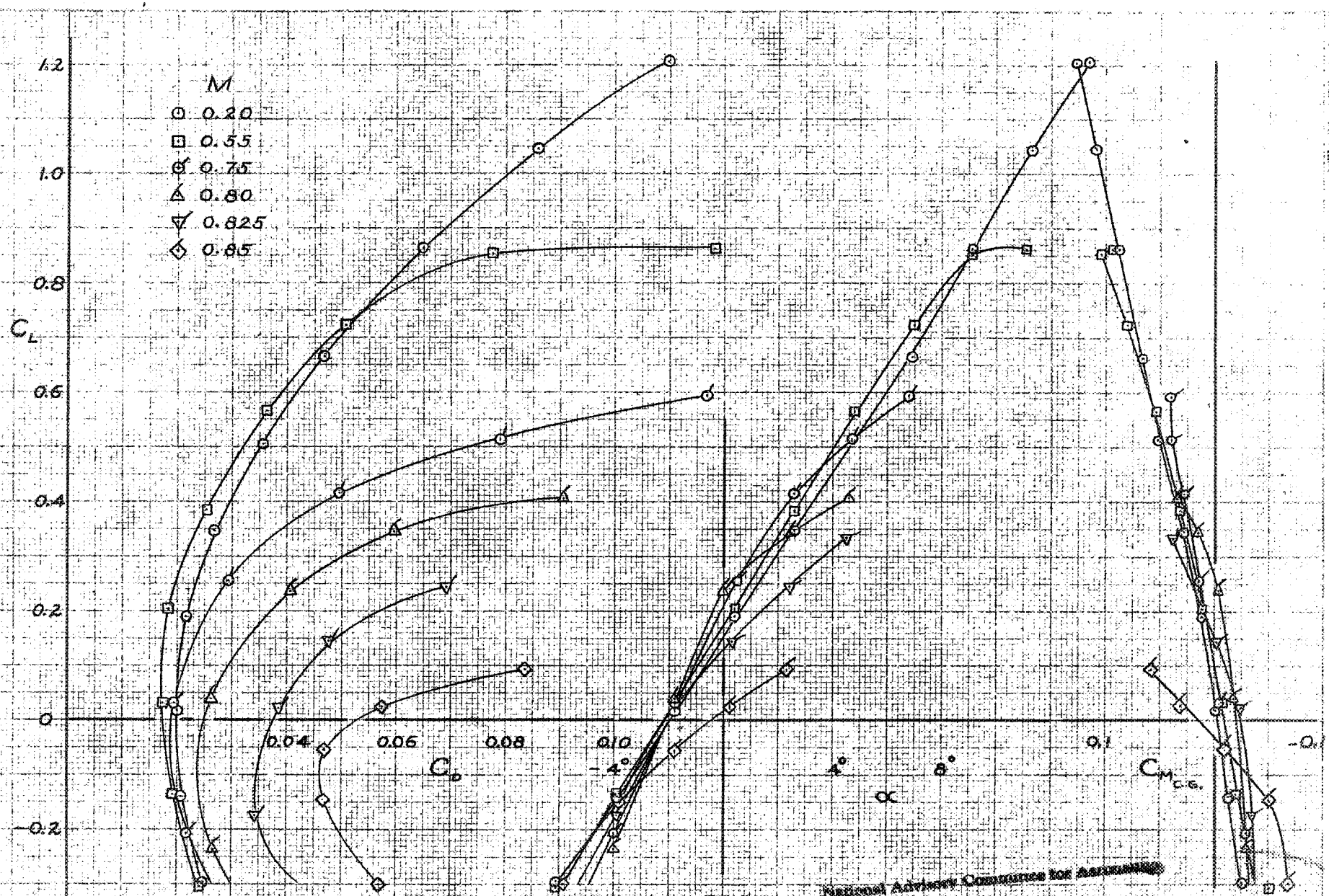

FIGURE 4.— LIFT, DRAG, AND PITCHING-MOMENT CHARACTERISTICS OF THE P-39N-1 MODEL WITHOUT A TAIL AT SEVERAL MACH NUMBERS.

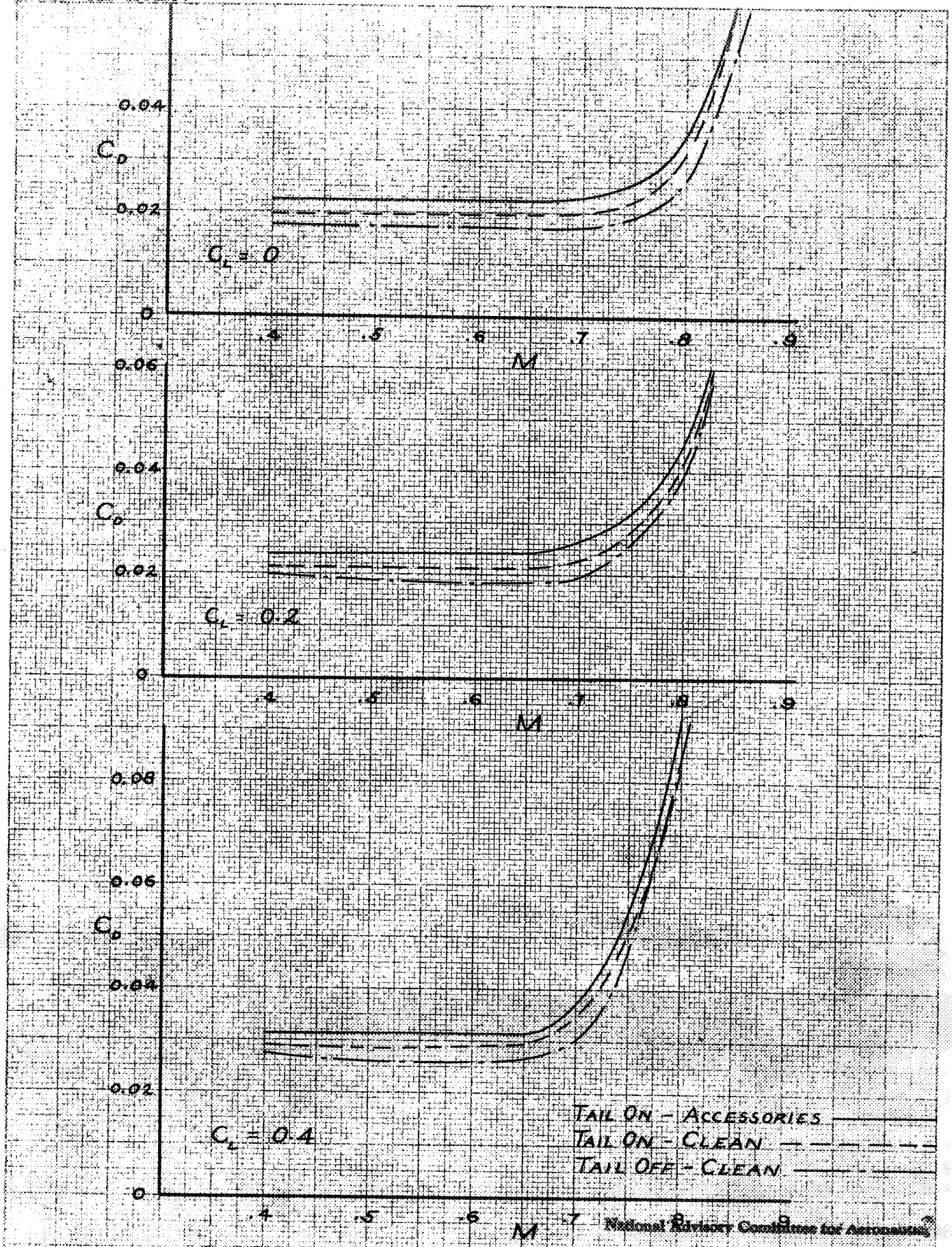

FIGURE 5 .- VARIATION OF DRAG COEFFICIENT WITH MACH

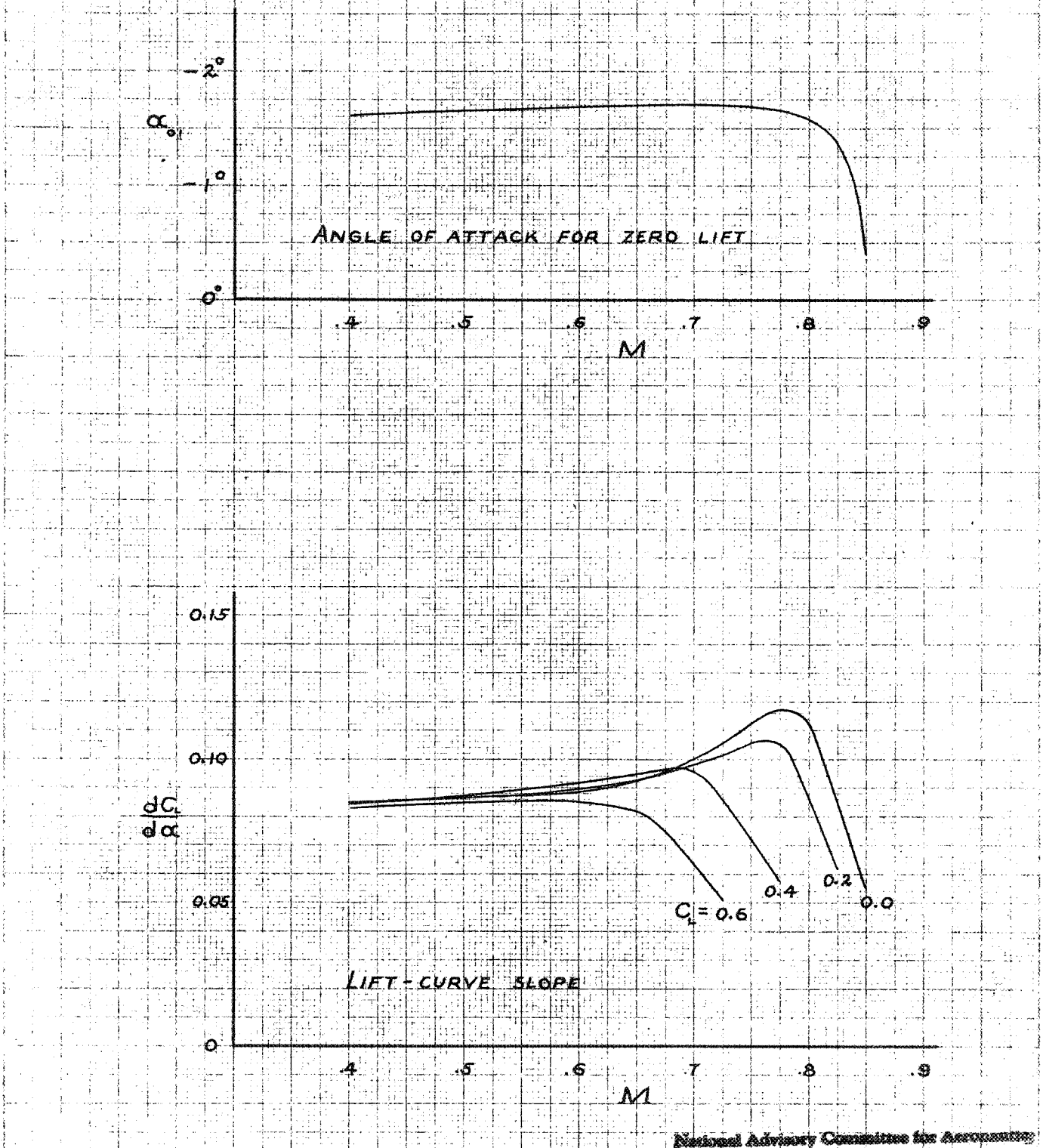

FIGURE 6 — VARIATION OF THE ANGLE OF ATTACK FOR ZERO LIFT AND THE SLOPE OF THE LIFT CURVE WITH MACH NUMBER. $\delta_e = 0°$; P-39N-1 MODEL.

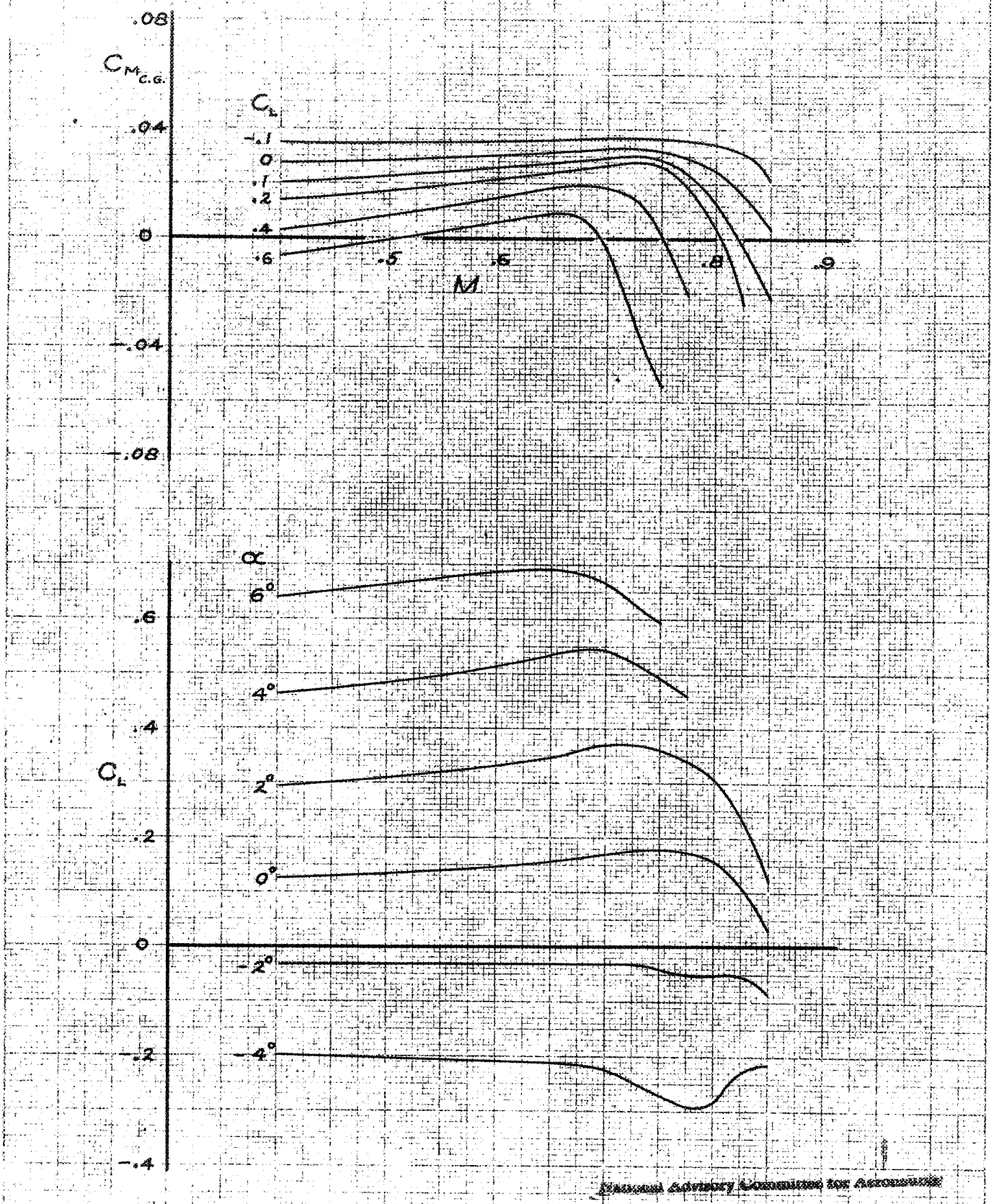

FIGURE 7. — THE VARIATION OF PITCHING-MOMENT COEFFICIENT AND LIFT COEFFICIENT WITH MACH NUMBER AT SEVERAL ATTITUDES. $\delta = 0°$, R 20N [illegible]

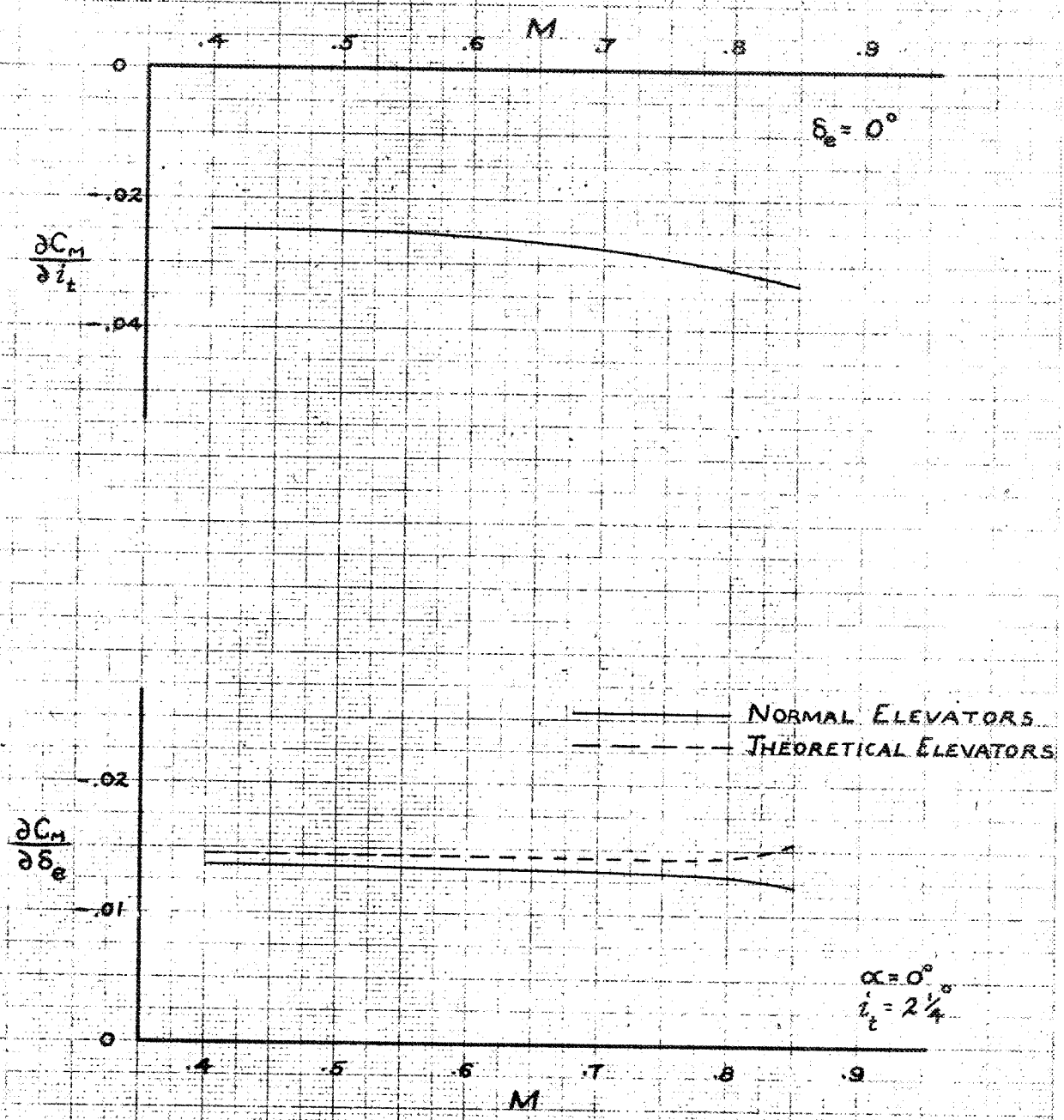

National Advisory Committee for Aeronautics

FIGURE 8.—VARIATION OF STABILIZER EFFECTIVENESS AND ELEVATOR EFFECTIVENESS WITH MACH NUMBER FOR THE P-39N-1 MODEL.

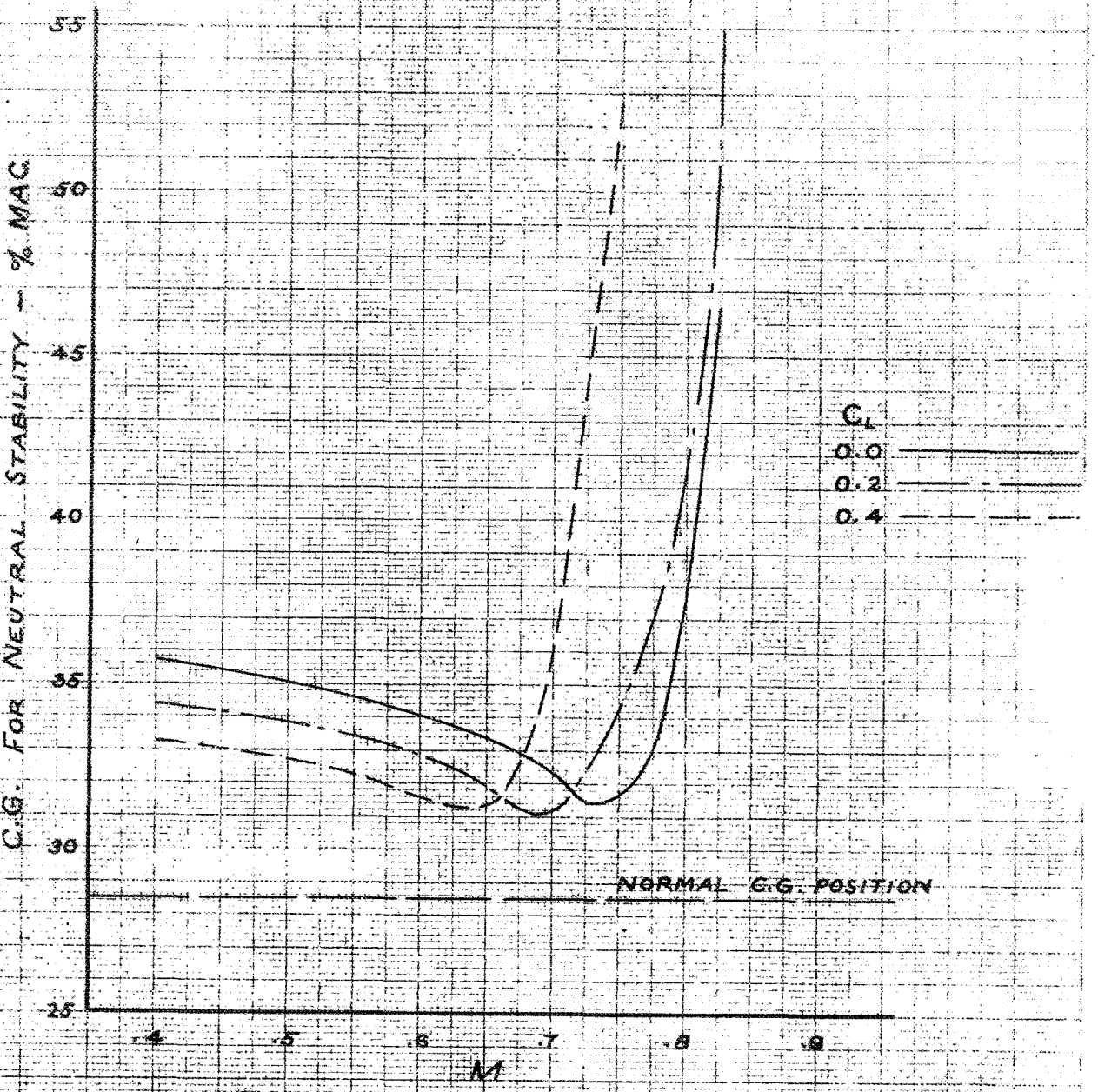

National Advisory Committee for Aeronautics

FIGURE 9. — VARIATION OF THE STICK-FIXED CENTER-OF-GRAVITY POSITION FOR NEUTRAL STABILITY WITH MACH NUMBER AT DIFFERENT VALUES OF LIFT COEFFICIENT. P-39N-1 MODEL.

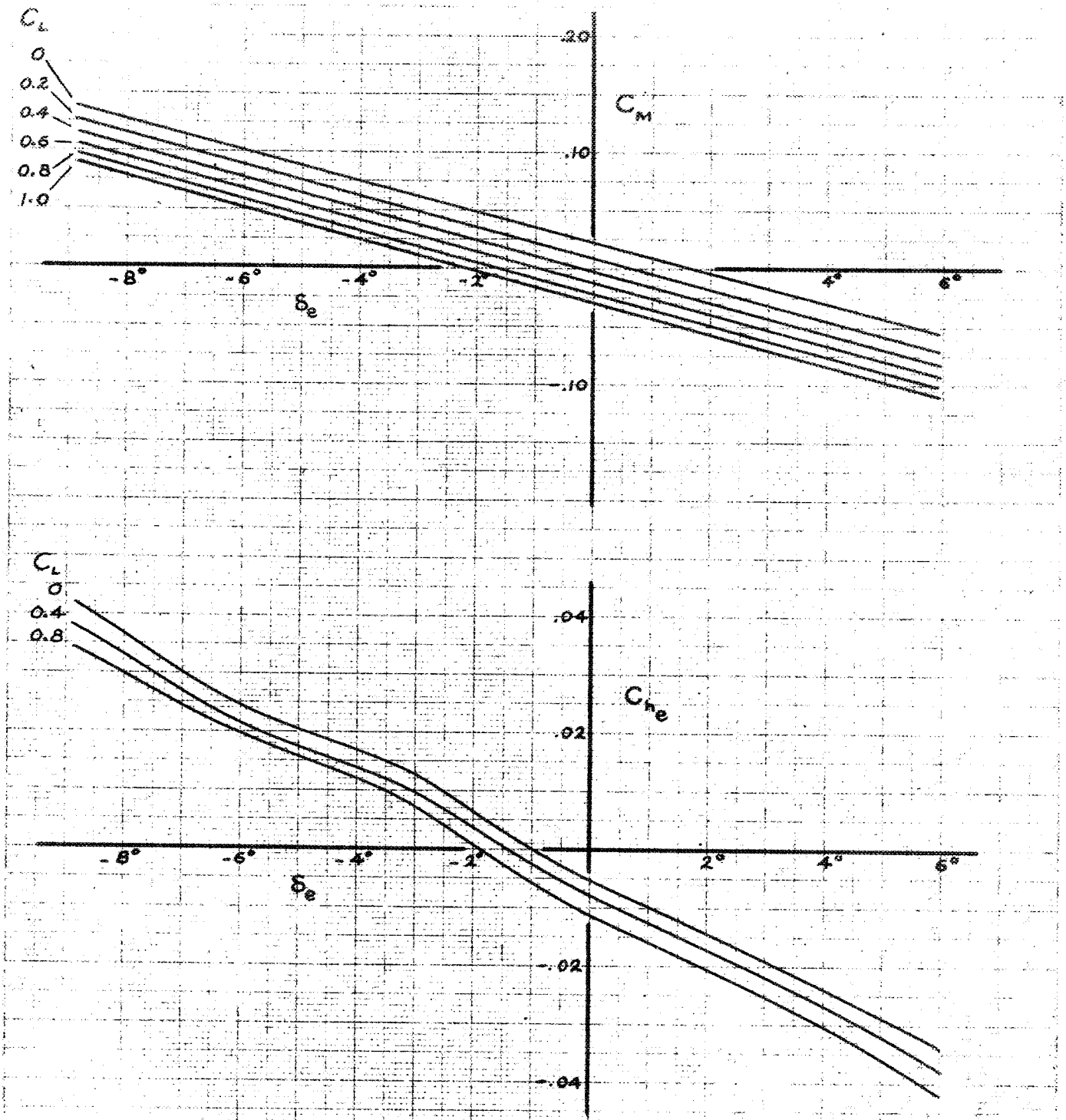

(a) $M = 0.4$

FIGURE 10.— VARIATION OF PITCHING-MOMENT AND ELEVATOR HINGE-MOMENT COEFFICIENTS WITH ELEVATOR ANGLE FOR CONSTANT LIFT COEFFICIENTS. NORMAL ELEVATORS; $i_t = 2\frac{1}{4}°$; $\delta_t = 0°$; P-39N-1 MODEL.

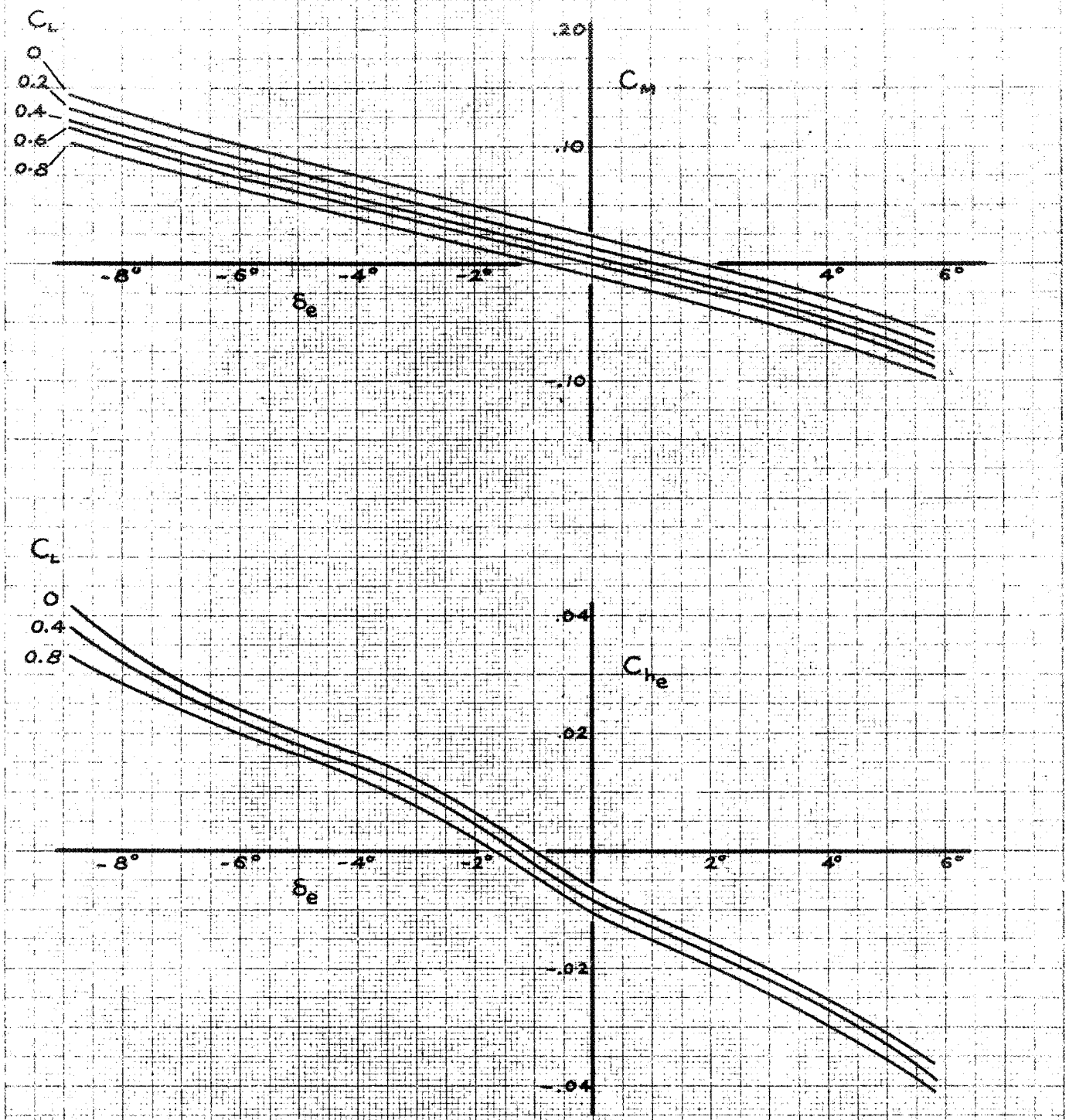

(b) $M = 0.55$

FIGURE 10.— CONTINUED. P-39N-1 MODEL.

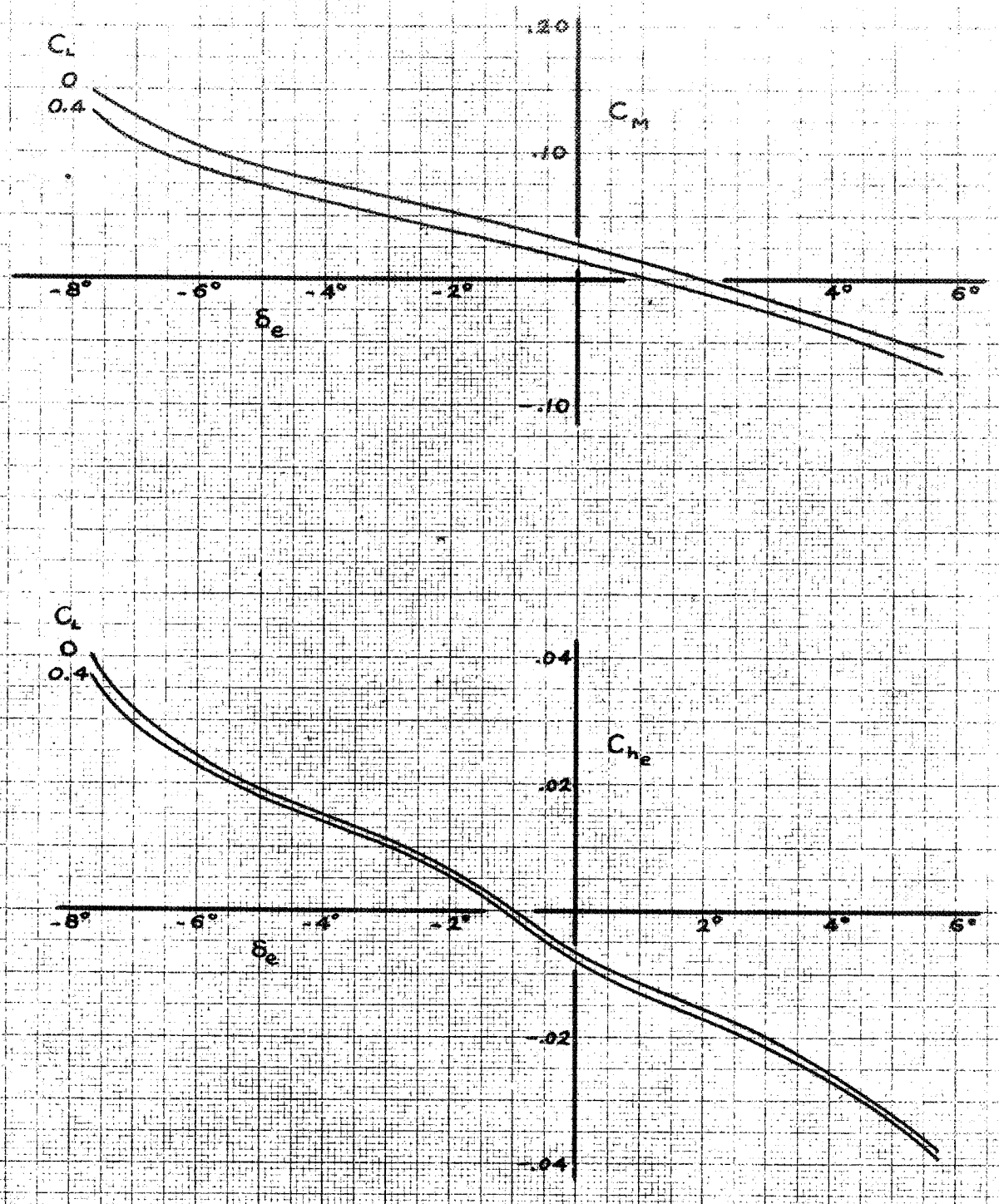

(c) $M = 0.65$

FIGURE 10.- CONTINUED. P-39N-1 MODEL.

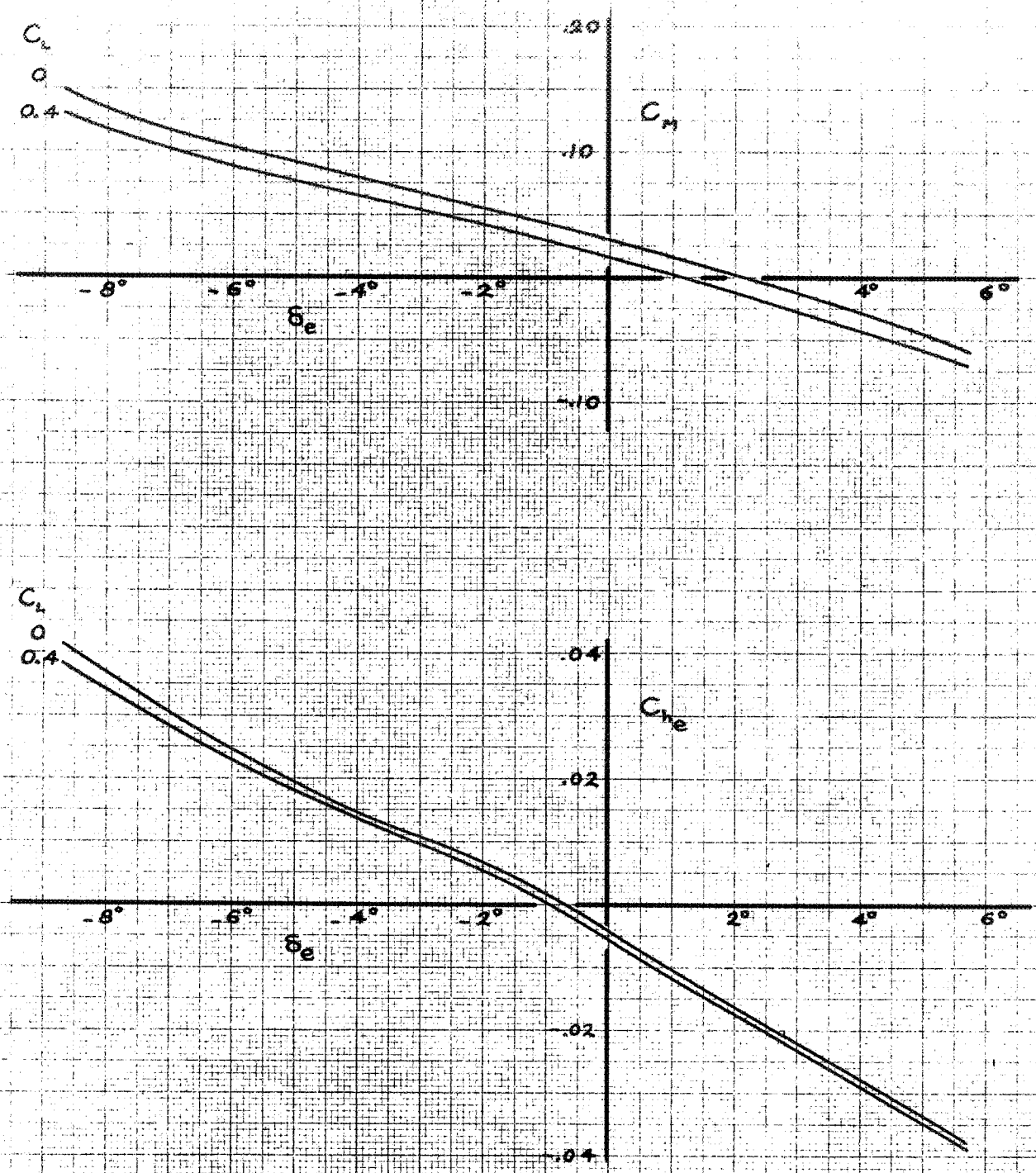

(d) $M = 0.70$

FIGURE 10 – CONTINUED. P-39N-1 MODEL.

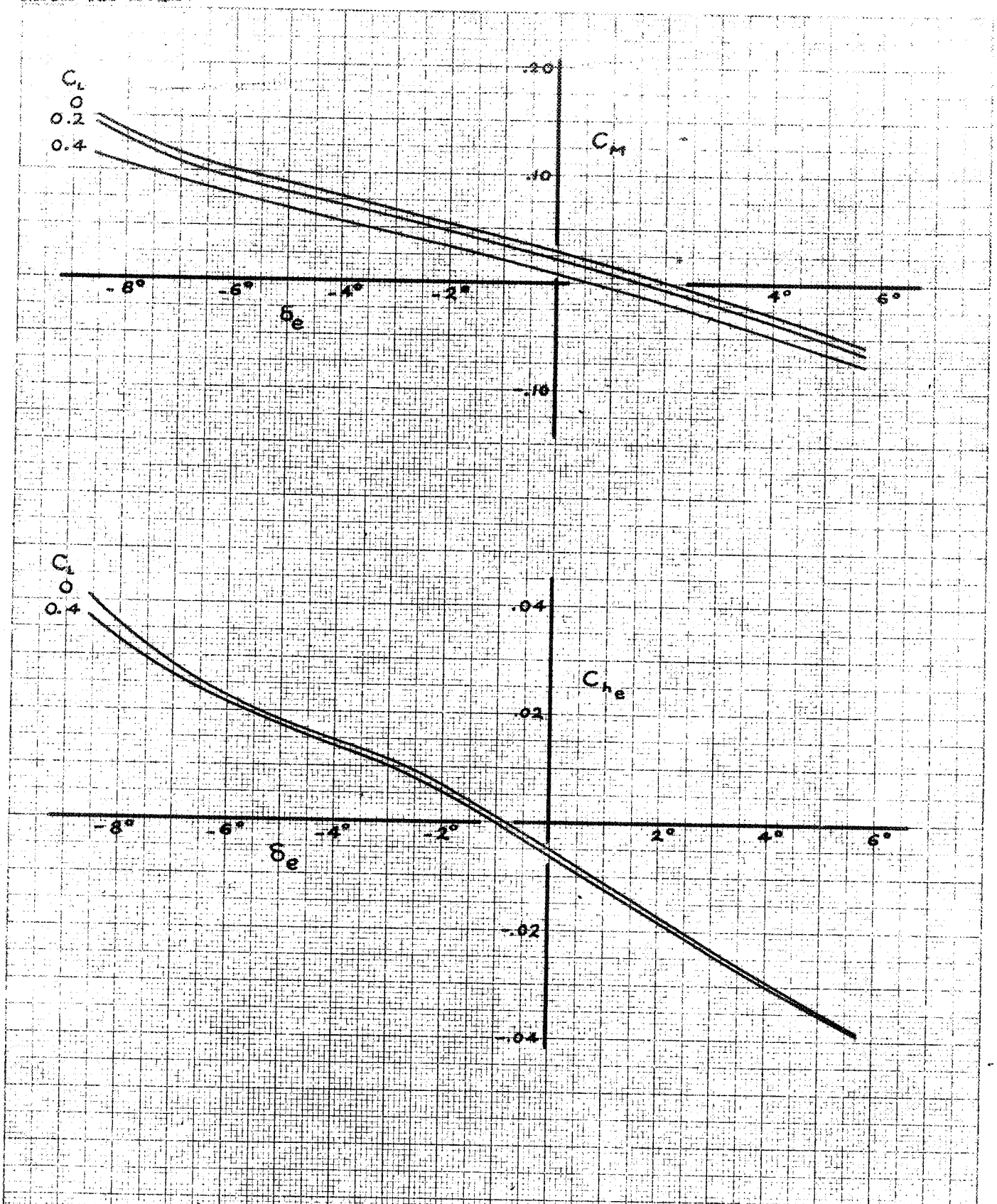

(e) $M = 0.725$

FIGURE 10.- CONTINUED. P-39N-1 MODEL.

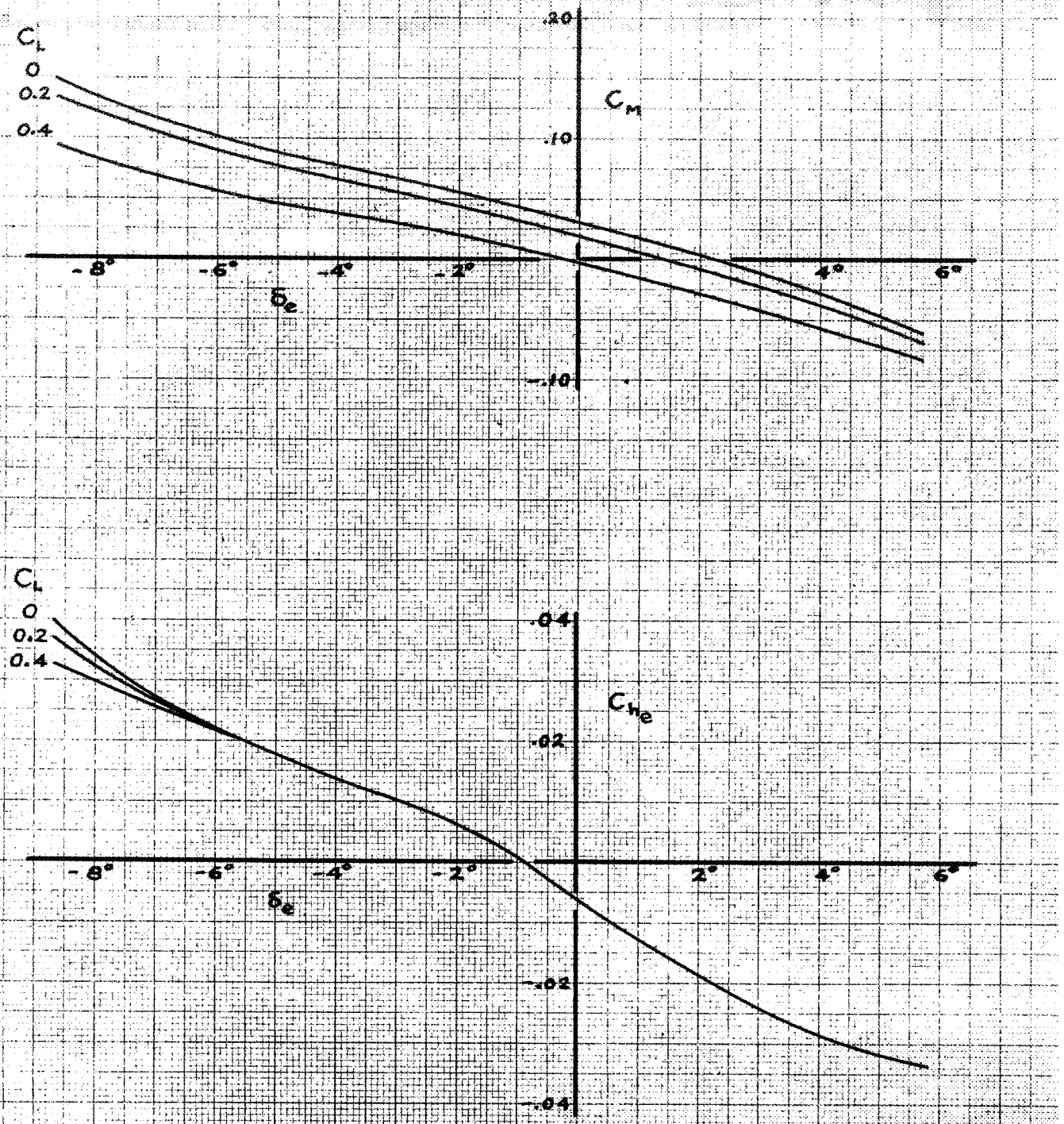

(f) $M = 0.75$

FIGURE 10.— CONTINUED. P-39N-1 MODEL.

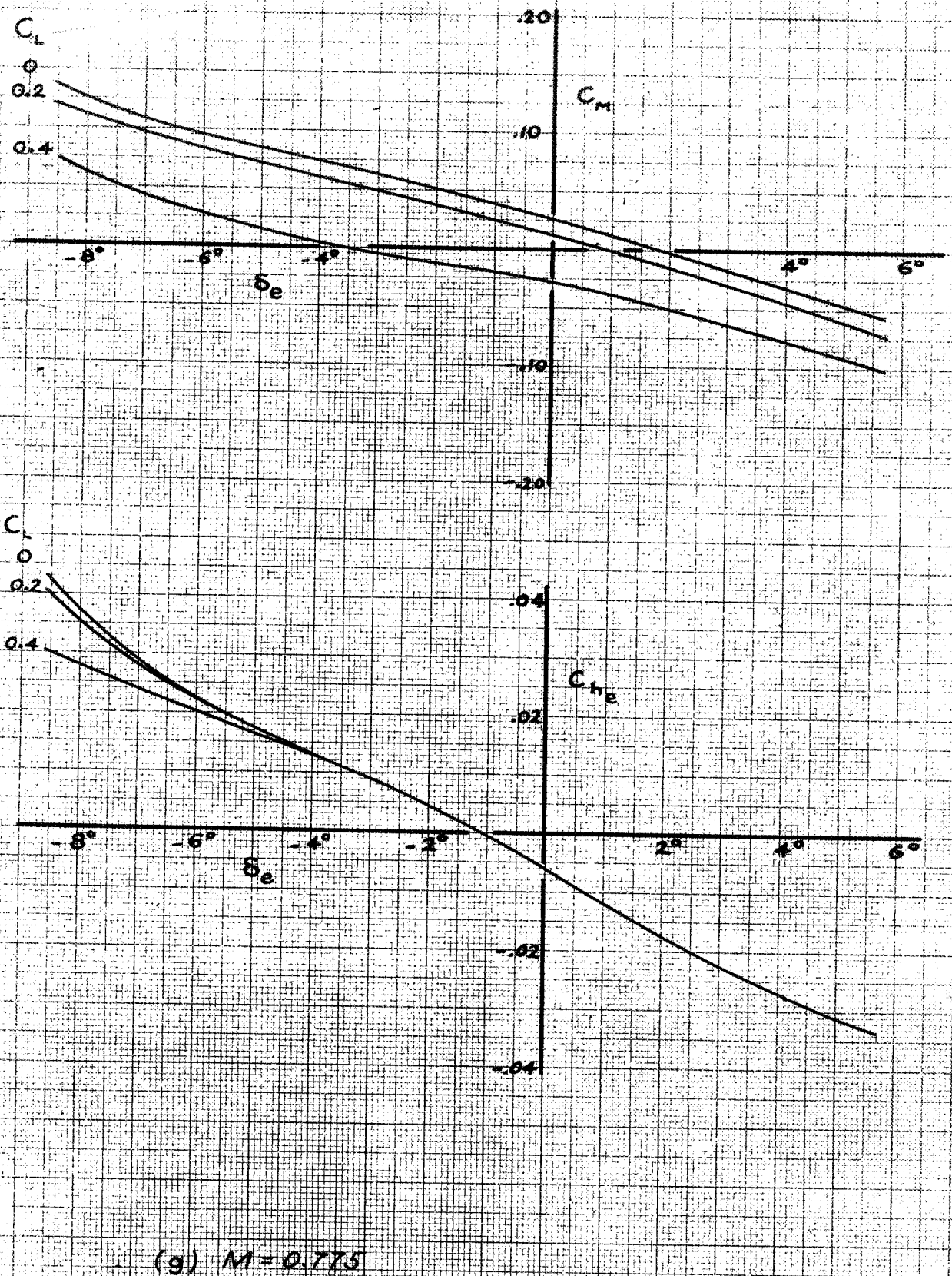

(g) $M = 0.775$

FIGURE 10.- CONTINUED. P-39N-1 MODEL.

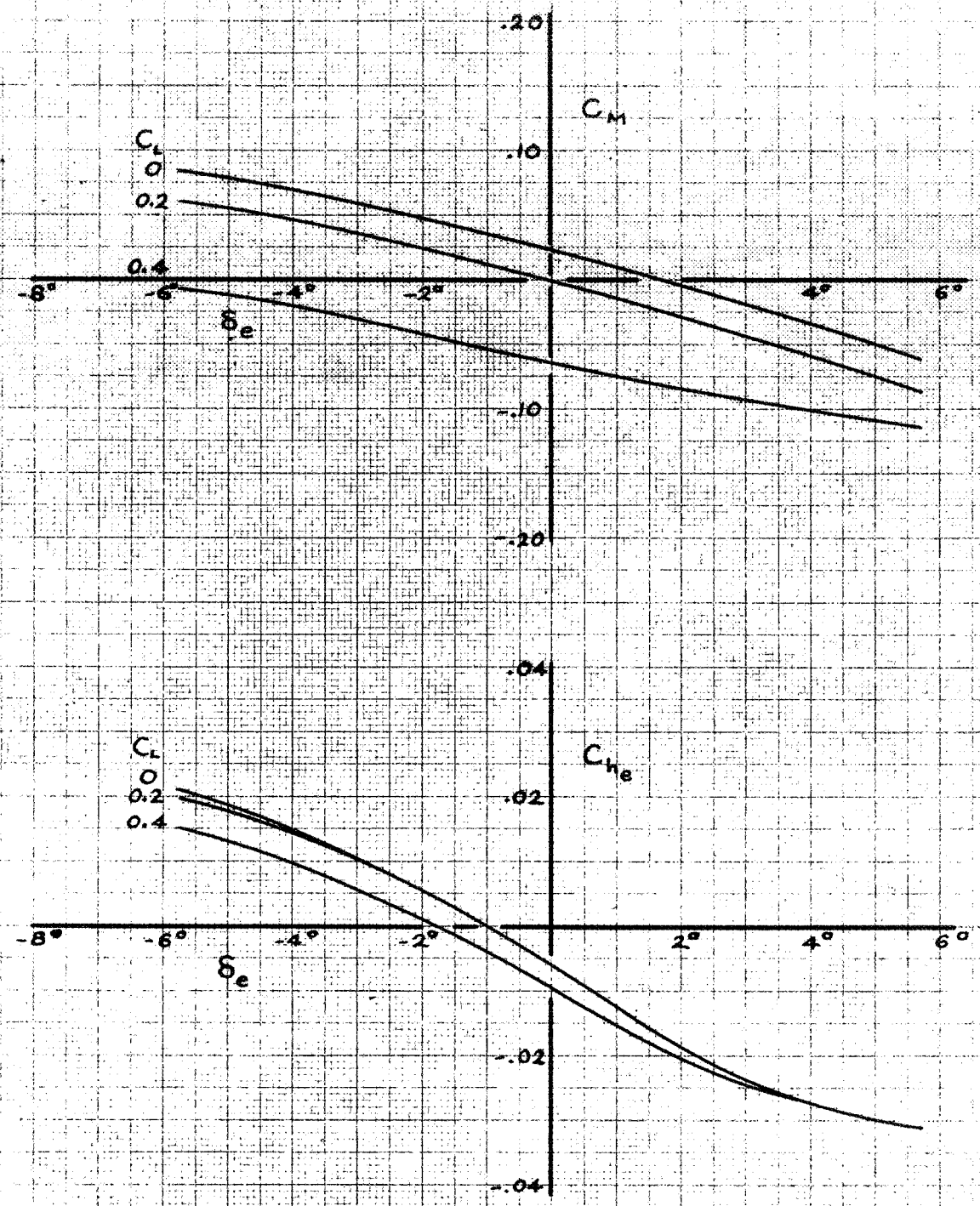

(h) $M = 0.80$

FIGURE 10.— CONTINUED. P-39N-1 MODEL.

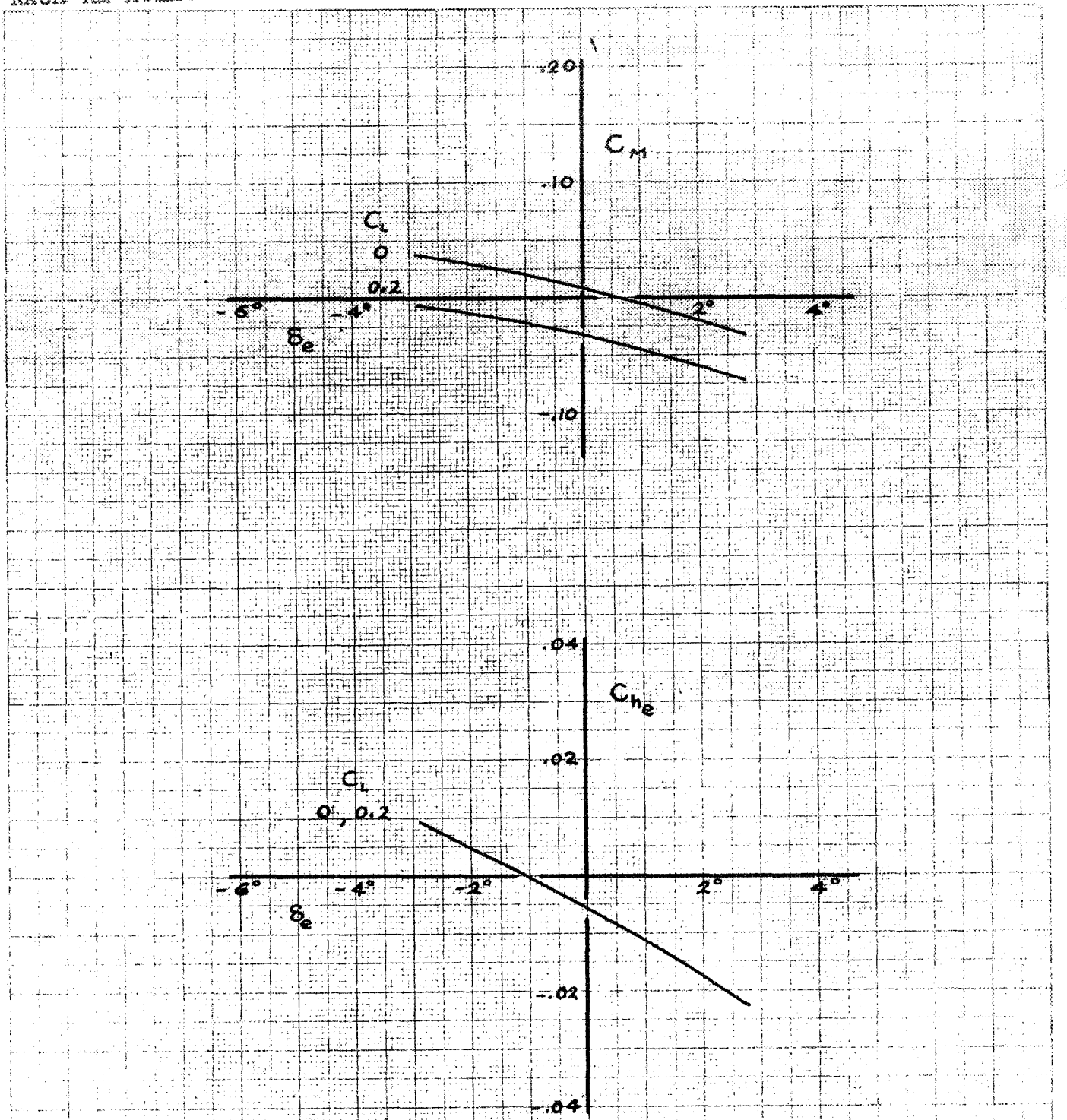

(i) $M = 0.825$

FIGURE 10.- CONTINUED. P-39N-1 MODEL.

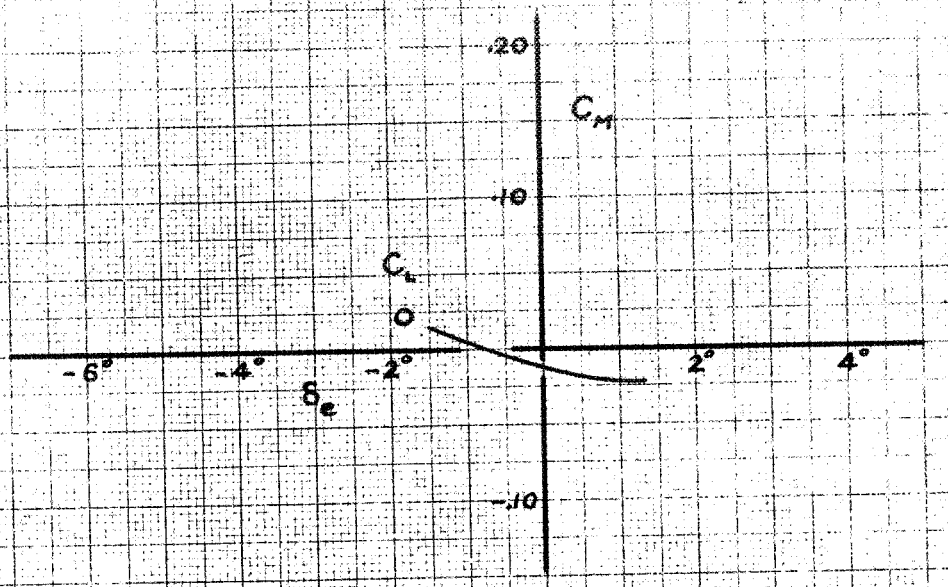

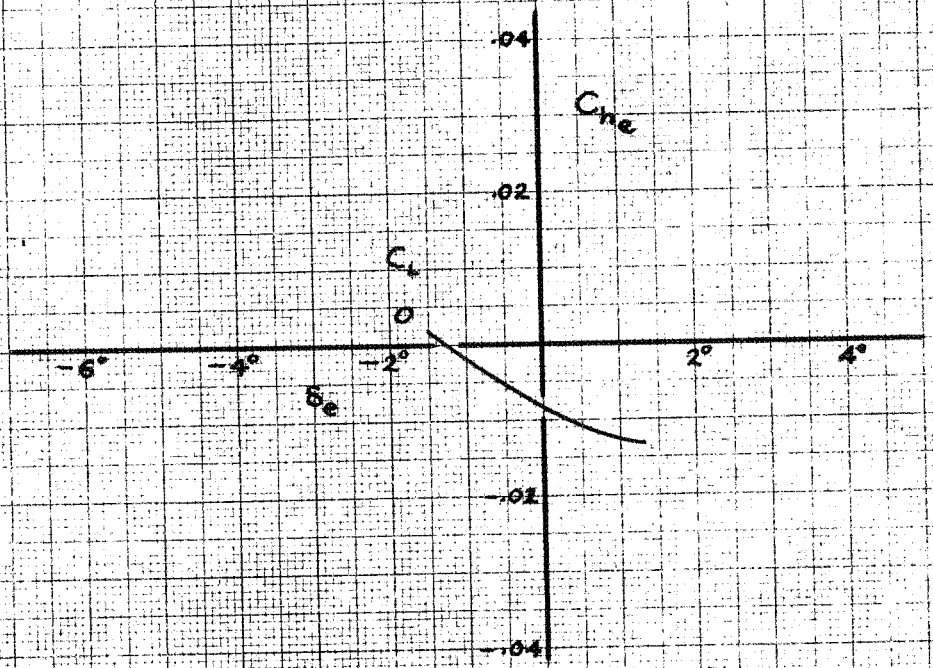

(j) $M = 0.85$

FIGURE 10.- CONCLUDED. P-39N-1 MODEL.

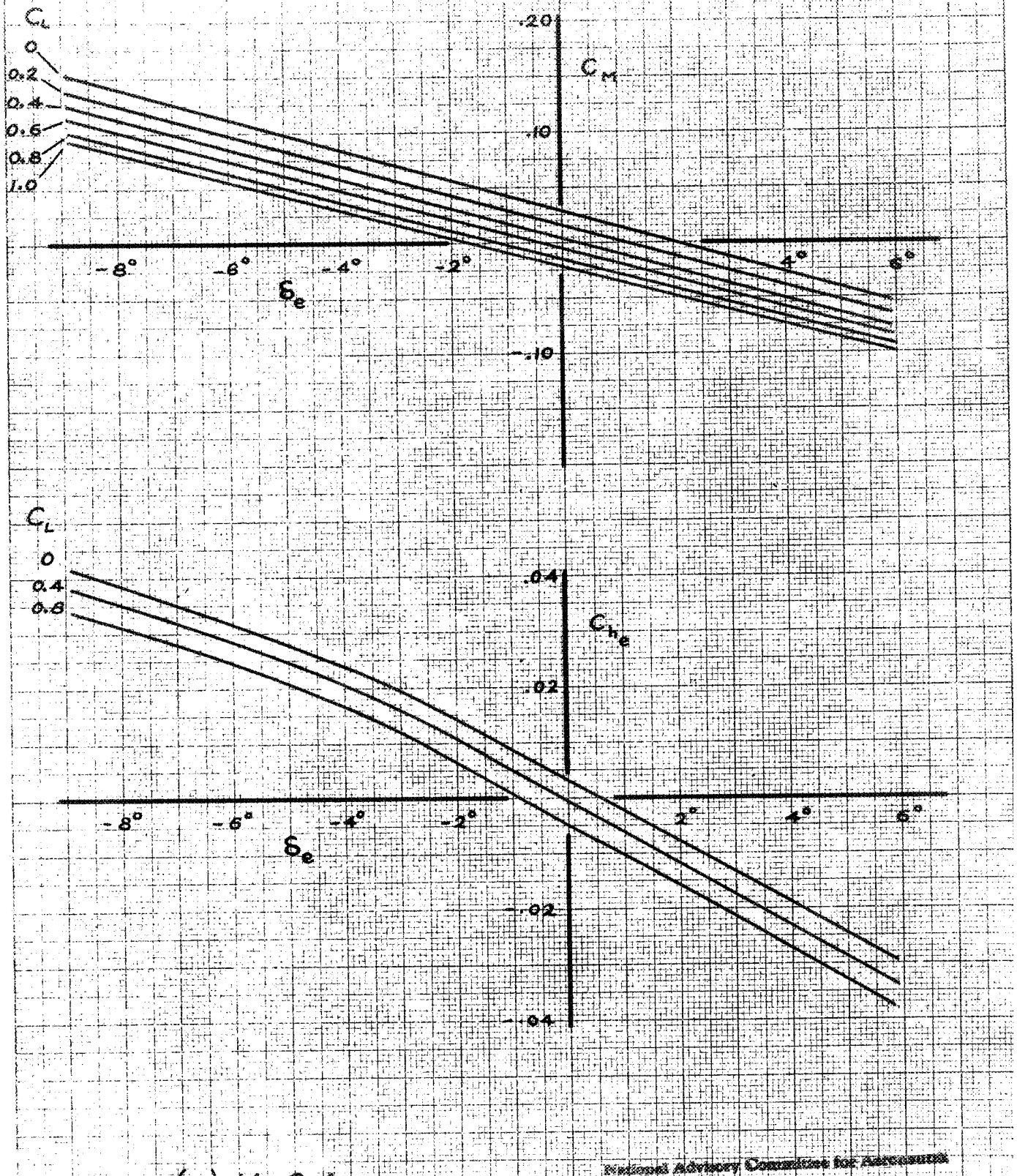

(a) $M = 0.4$

FIGURE 11.—VARIATION OF PITCHING-MOMENT AND ELEVATOR HINGE-MOMENT COEFFICIENTS WITH ELEVATOR ANGLE FOR CONSTANT LIFT COEFFICIENTS. THEORETICAL ELEVATORS; $i_t = 2\frac{1}{4}°$; $\delta_t = 0°$; P-39N-1 MODEL.

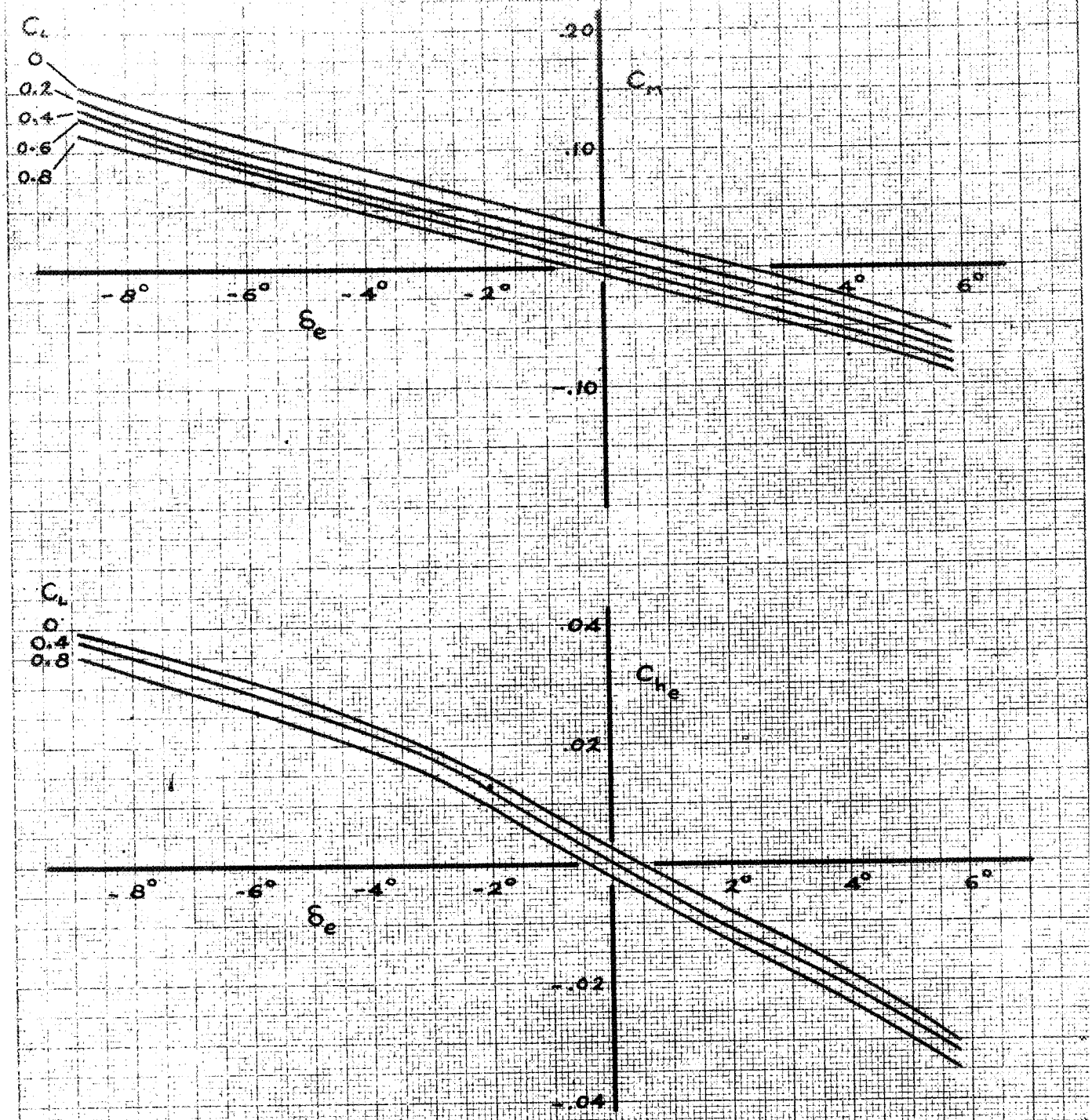

(b) $M = 0.55$

FIGURE 11.- CONTINUED. P-39N-1 MODEL.

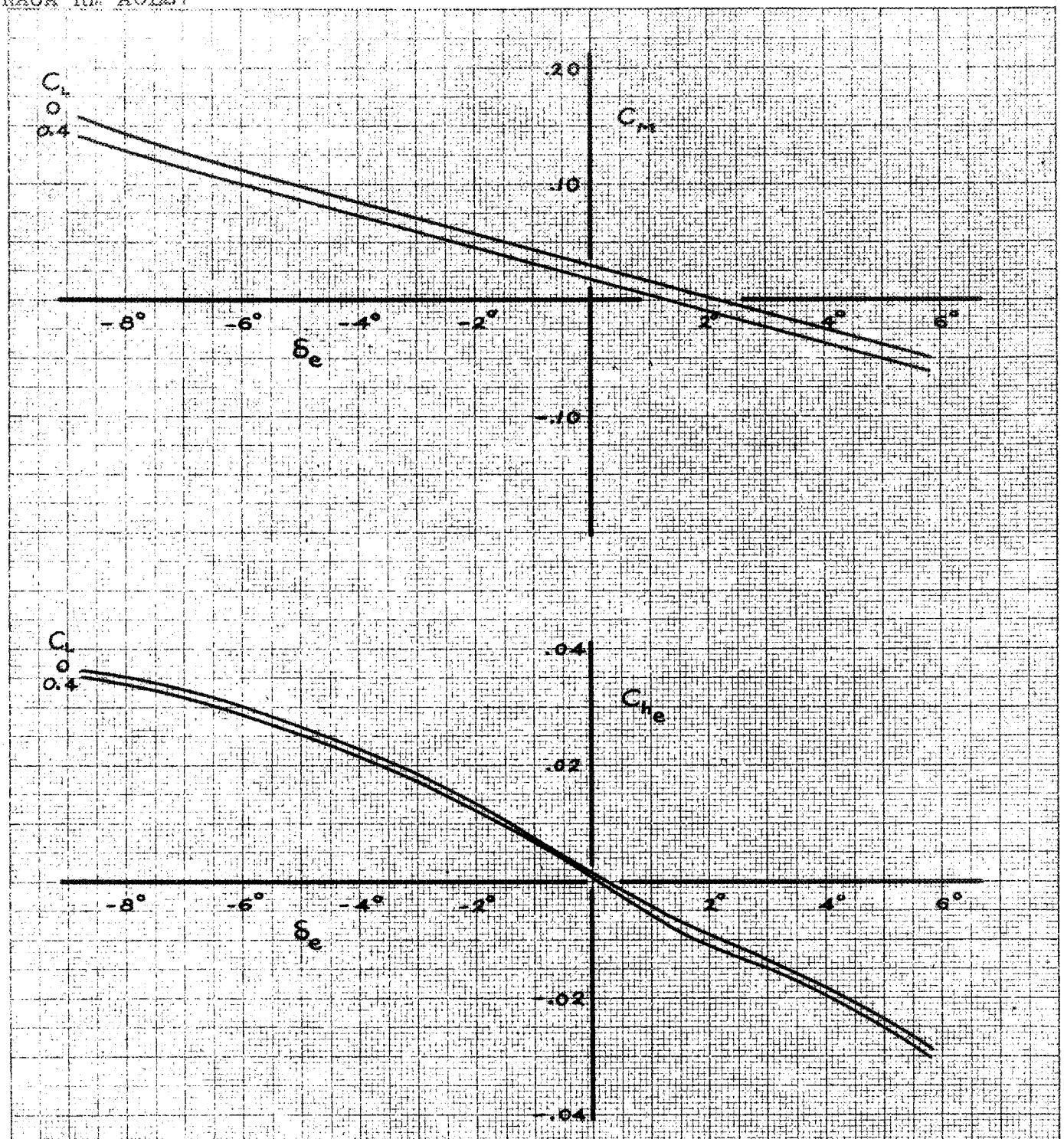

(c) $M = 0.65$

FIGURE 11.- CONTINUED. P-39N-1 MODEL.

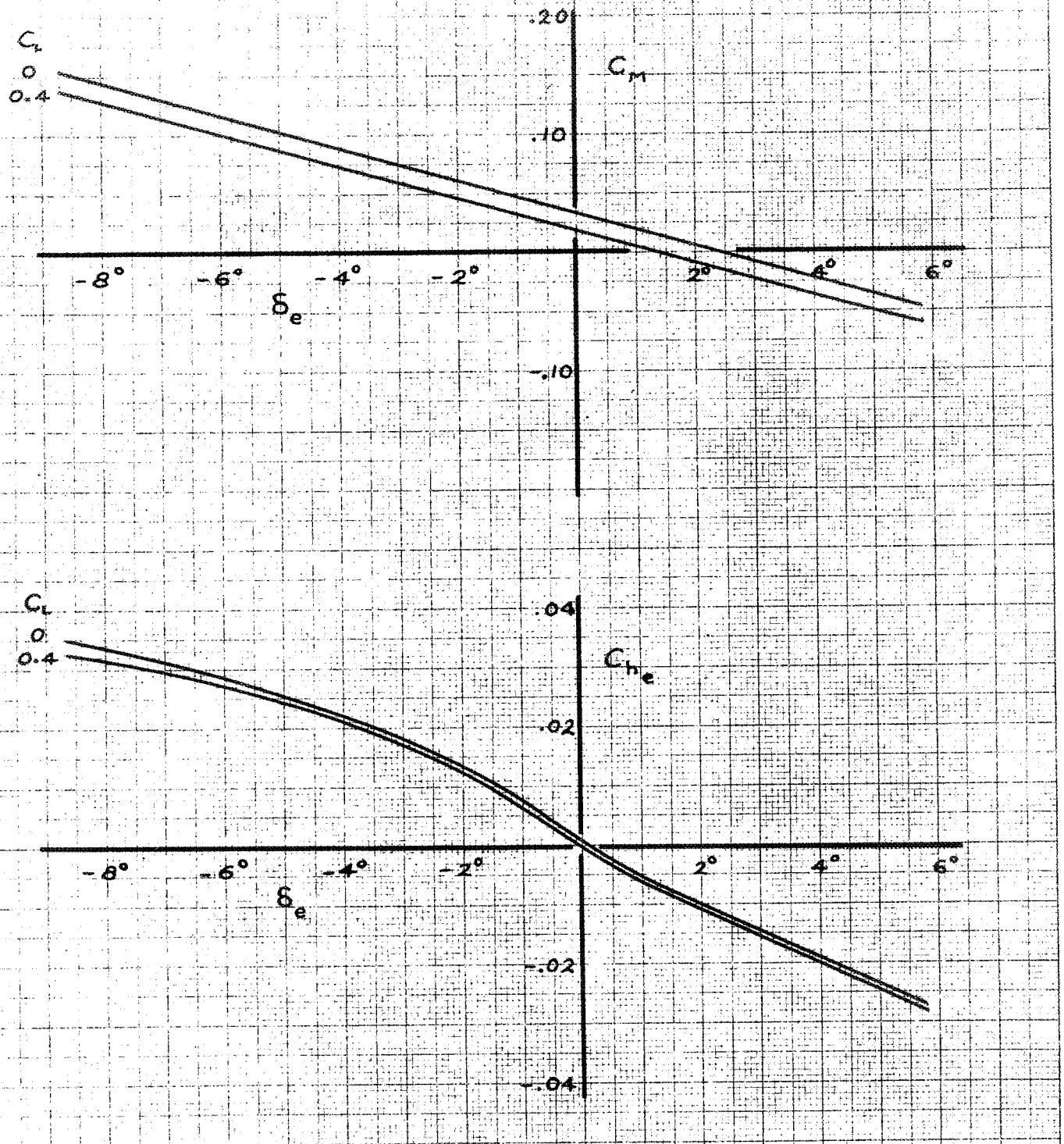

(d) $M = 0.70$

FIGURE 11 .- CONTINUED. P-39N-1 MODEL.

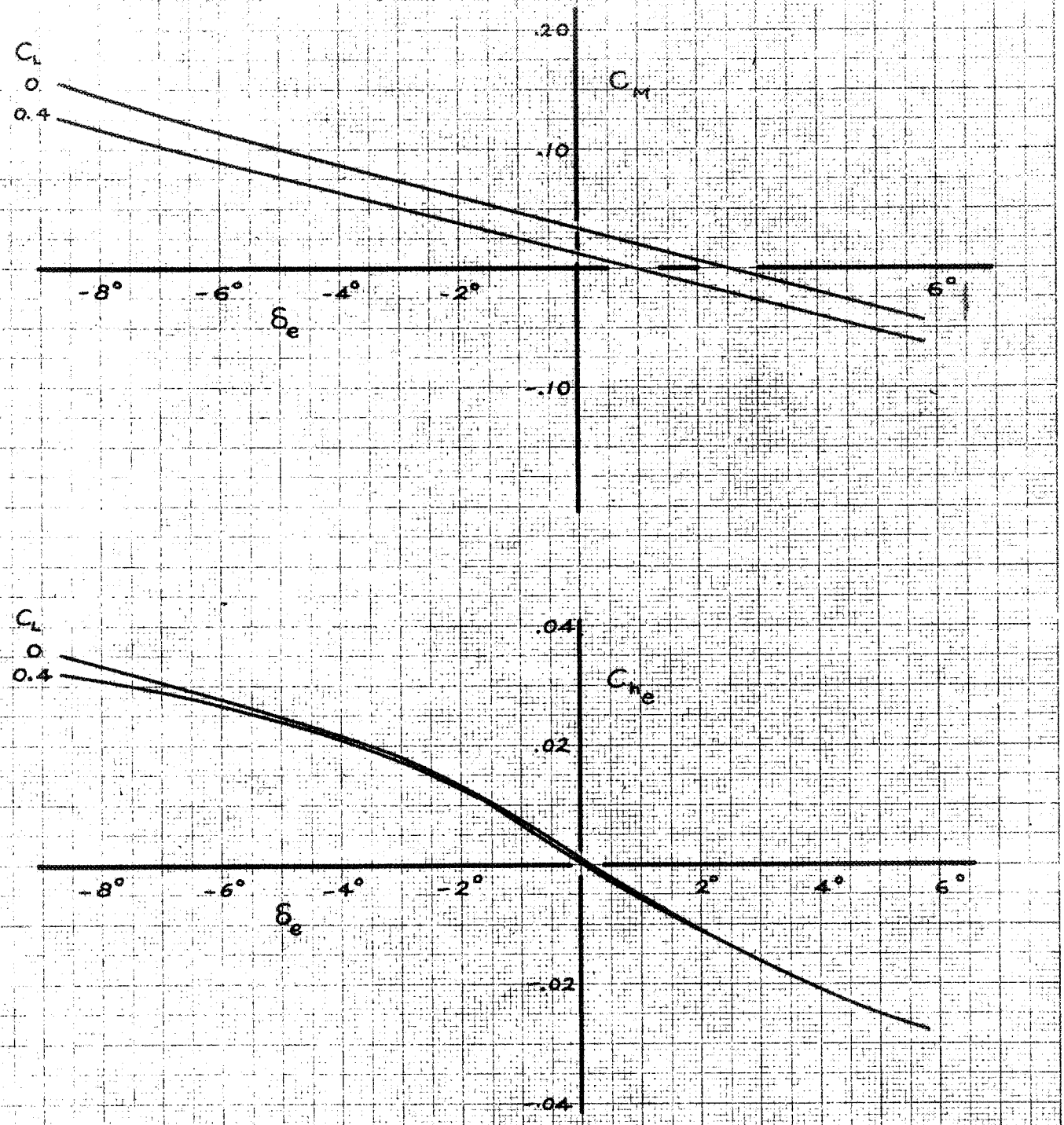

(e) $M = 0.725$

FIGURE 11.- CONTINUED. P-39N-1 MODEL.

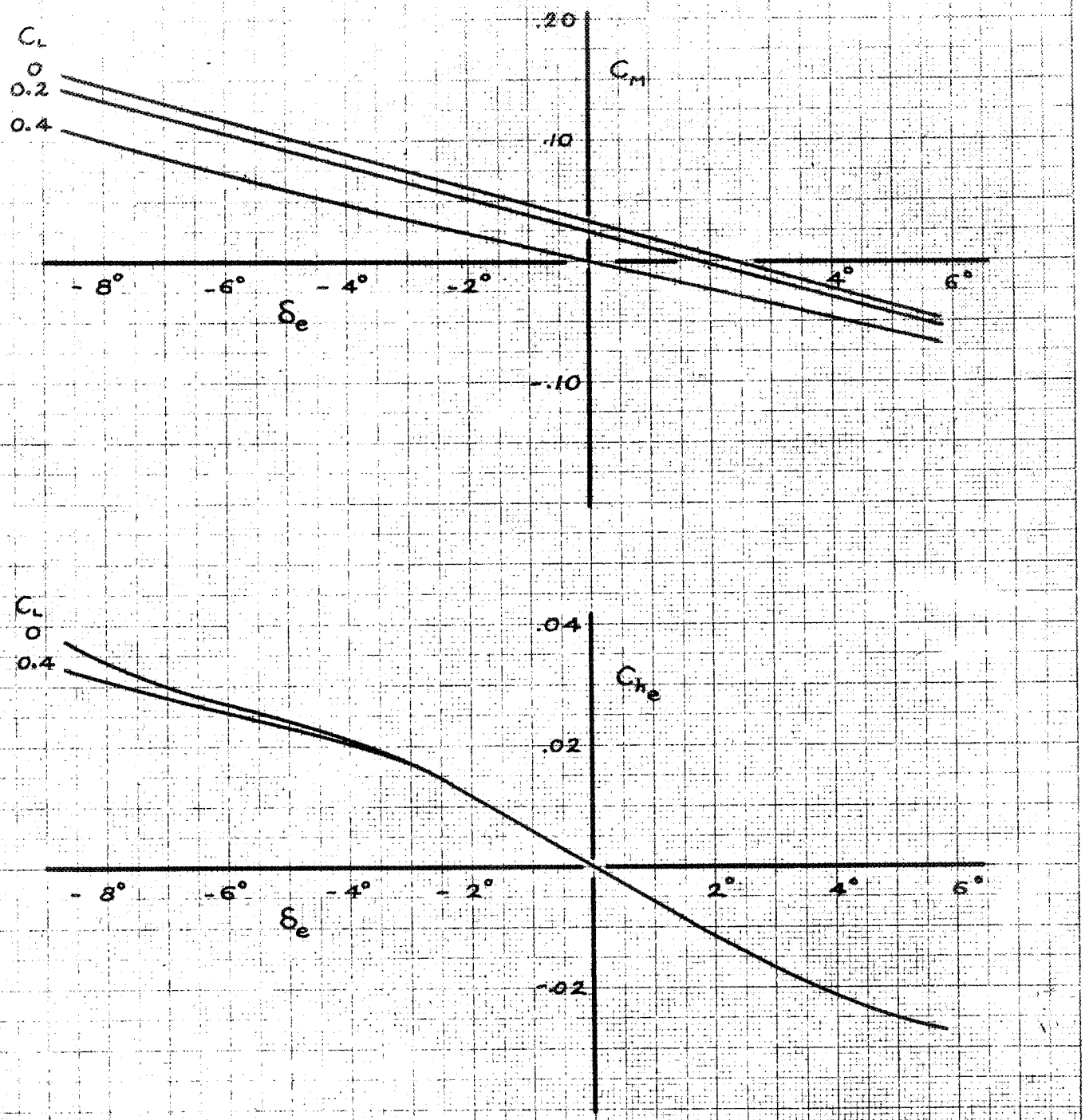

(f) $M = 0.75$

FIGURE 11.- CONTINUED. P-39N-1 MODEL.

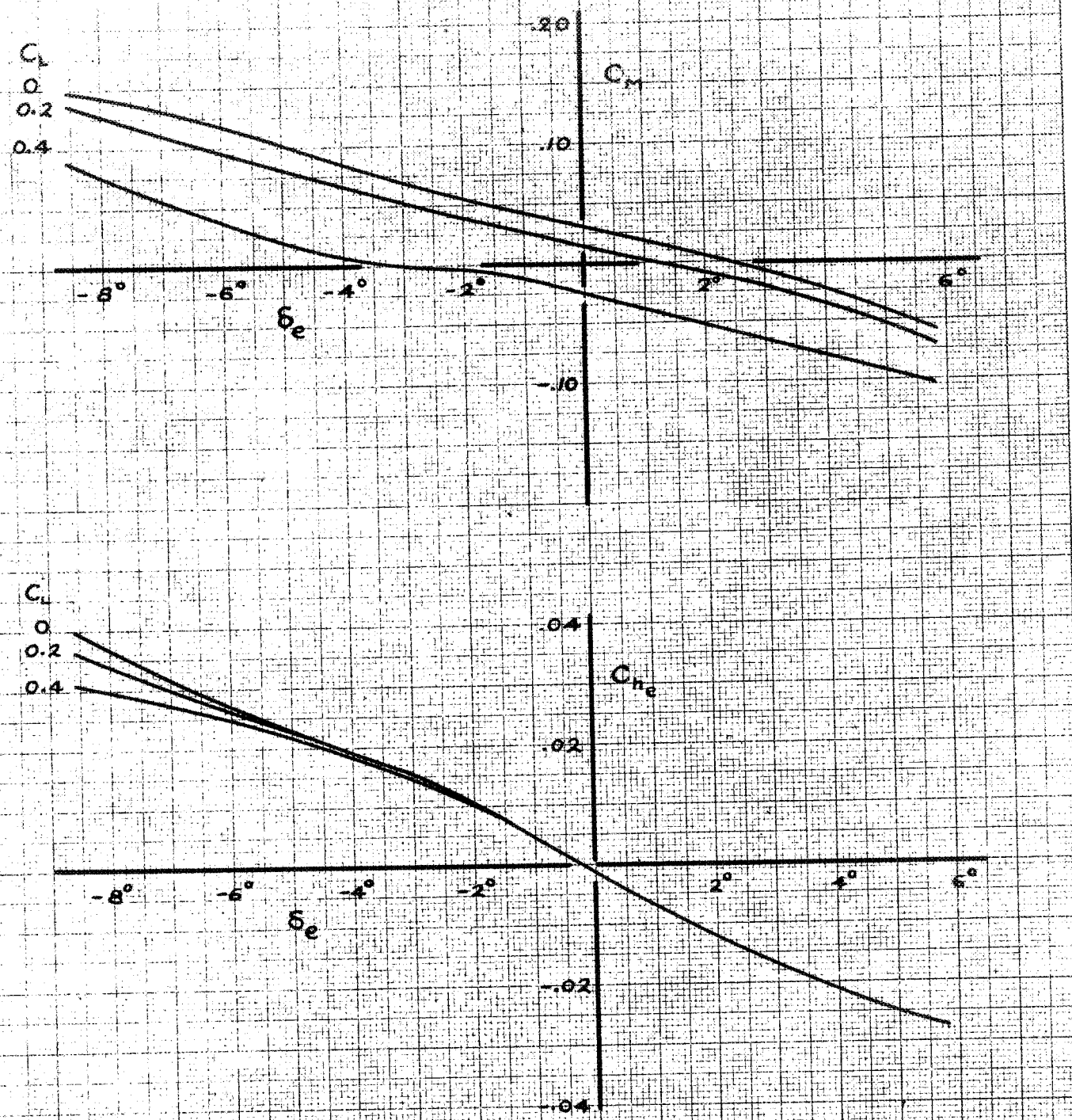

(g) $M = 0.775$

FIGURE 11.- CONTINUED. P-39N-1 MODEL.

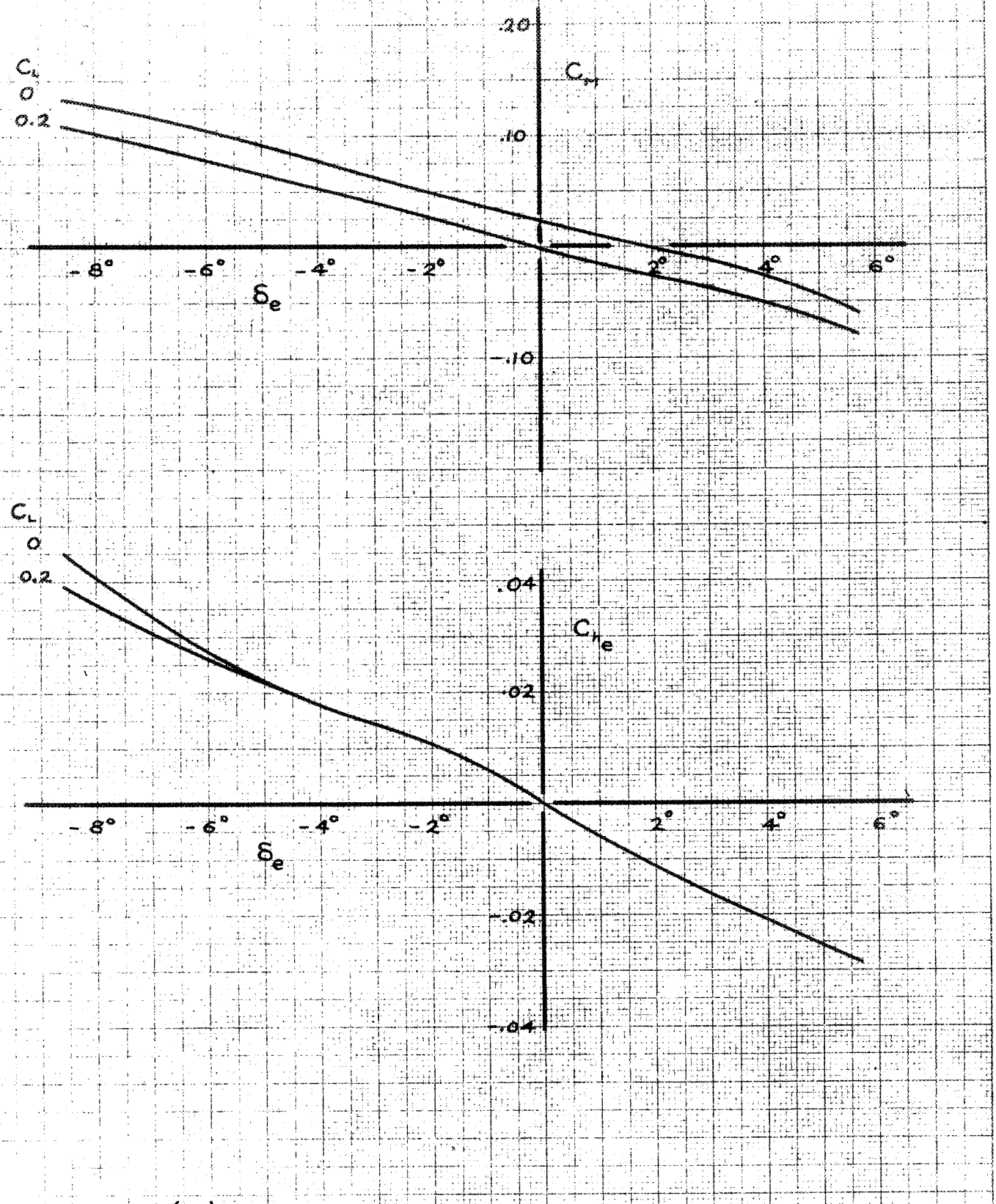

(h) $M = 0.80$

FIGURE 11.—CONTINUED. P-39N-1 MODEL.

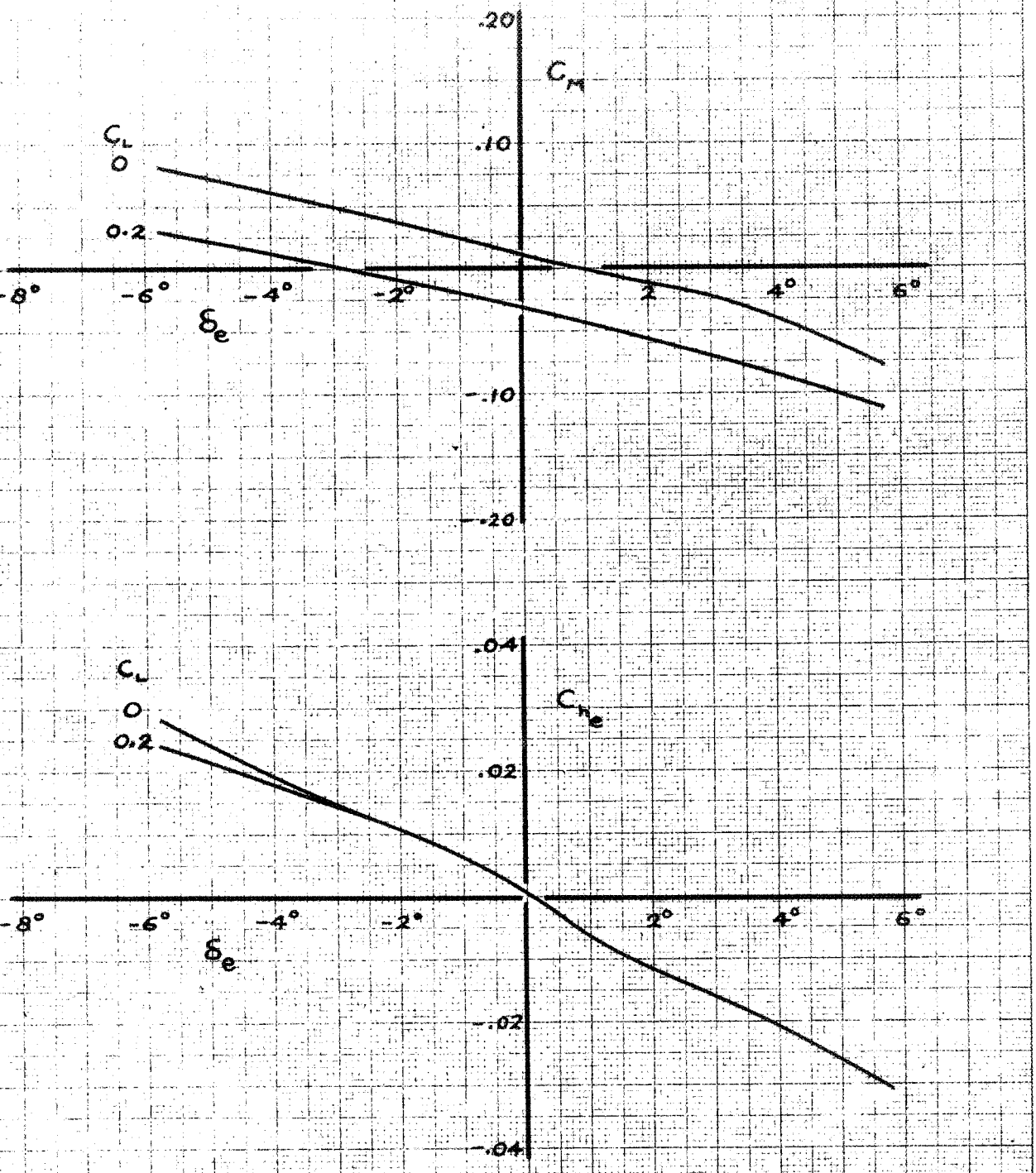

(i) $M = 0.825$

FIGURE 11.- CONTINUED. P-39N-1 MODEL.

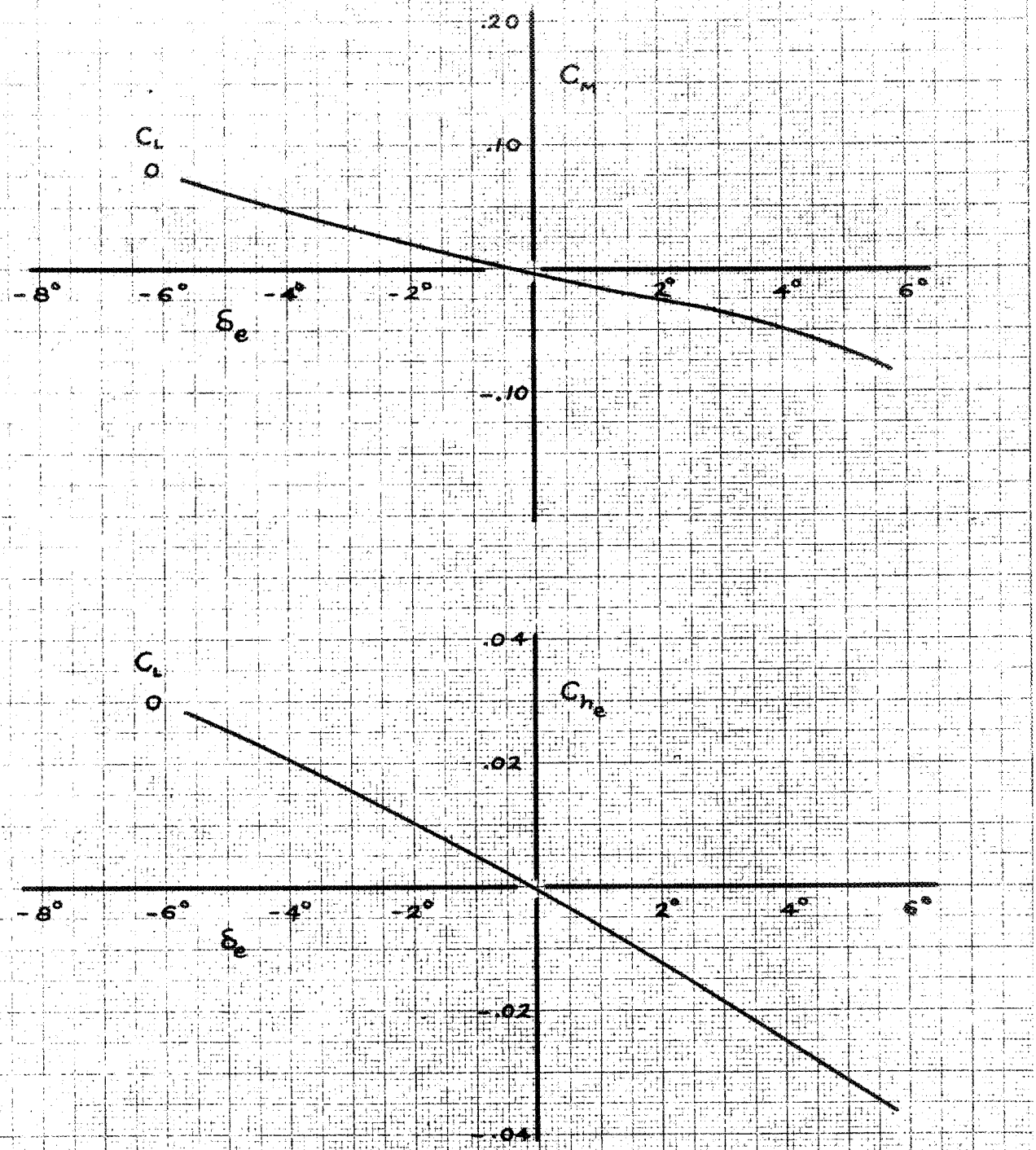

(j) $M = 0.85$

FIGURE 11.- CONCLUDED. P-39N-1 MODEL

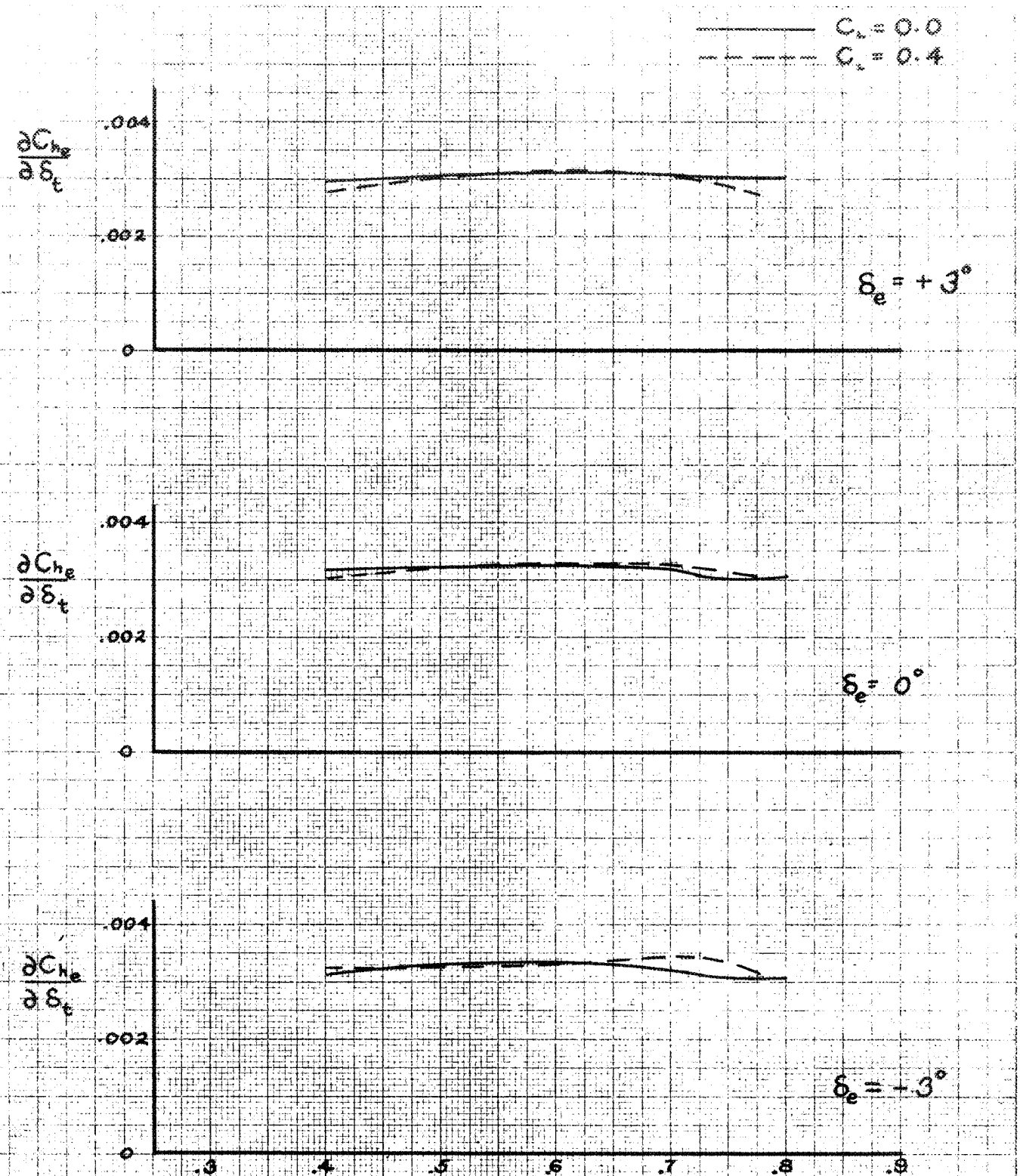

National Advisory Committee for Aeronautics

FIGURE 12. — VARIATION OF ELEVATOR TRIM-TAB EFFECTIVENESS WITH MACH NUMBER AT DIFFERENT ELEVATOR ANGLES AND LIFT COEFFICIENTS. P-38N-1 MODEL.

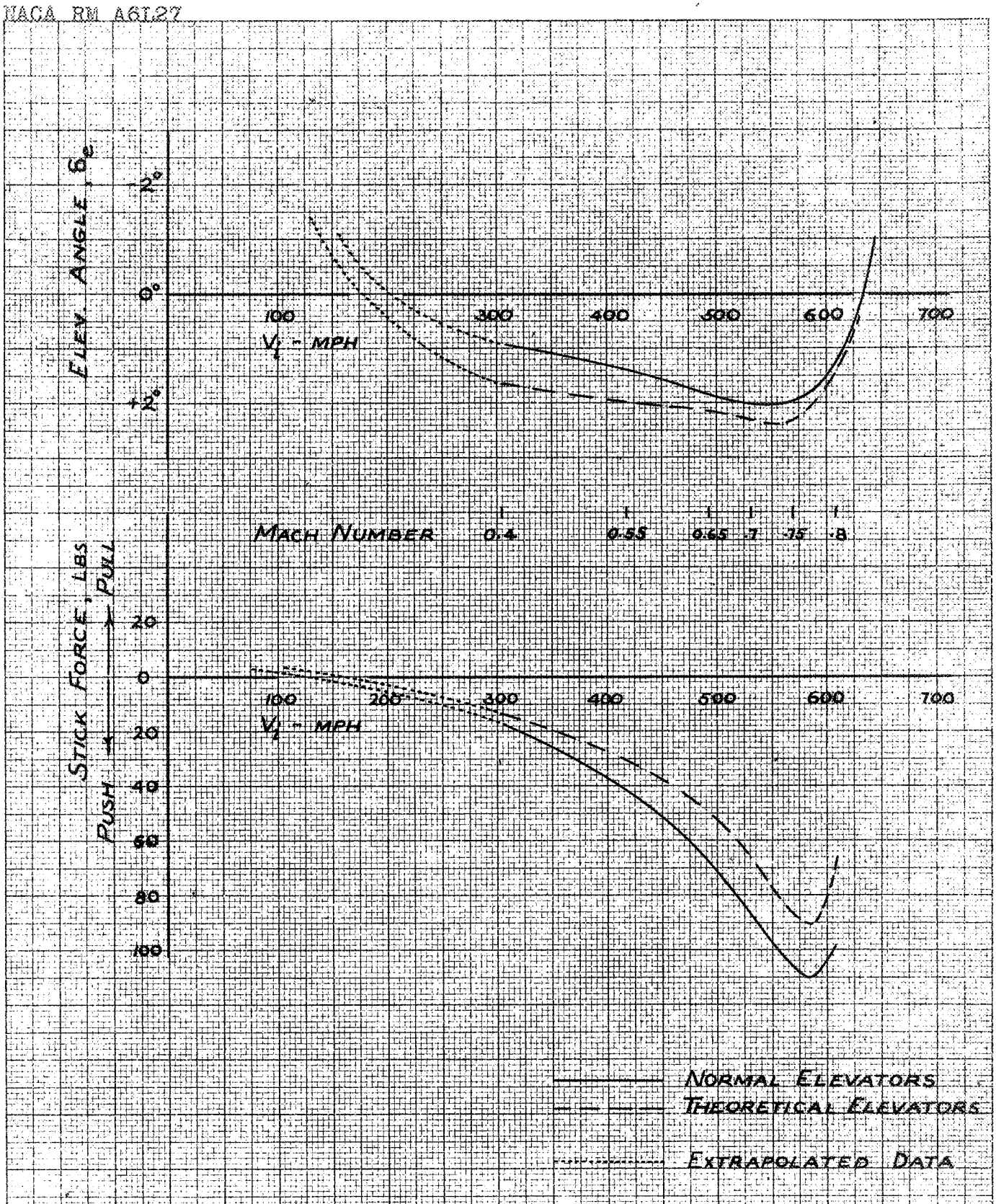

(a) SEA LEVEL

FIGURE 13 - VARIATION OF ELEVATOR ANGLE AND STICK FORCE WITH INDICATED AIRSPEED FOR BALANCE OF THE P-38N-1 AIRPLANE IN LEVEL FLIGHT. AS PREDICTED FROM TESTS OF A 0.35-SCALE MODEL.

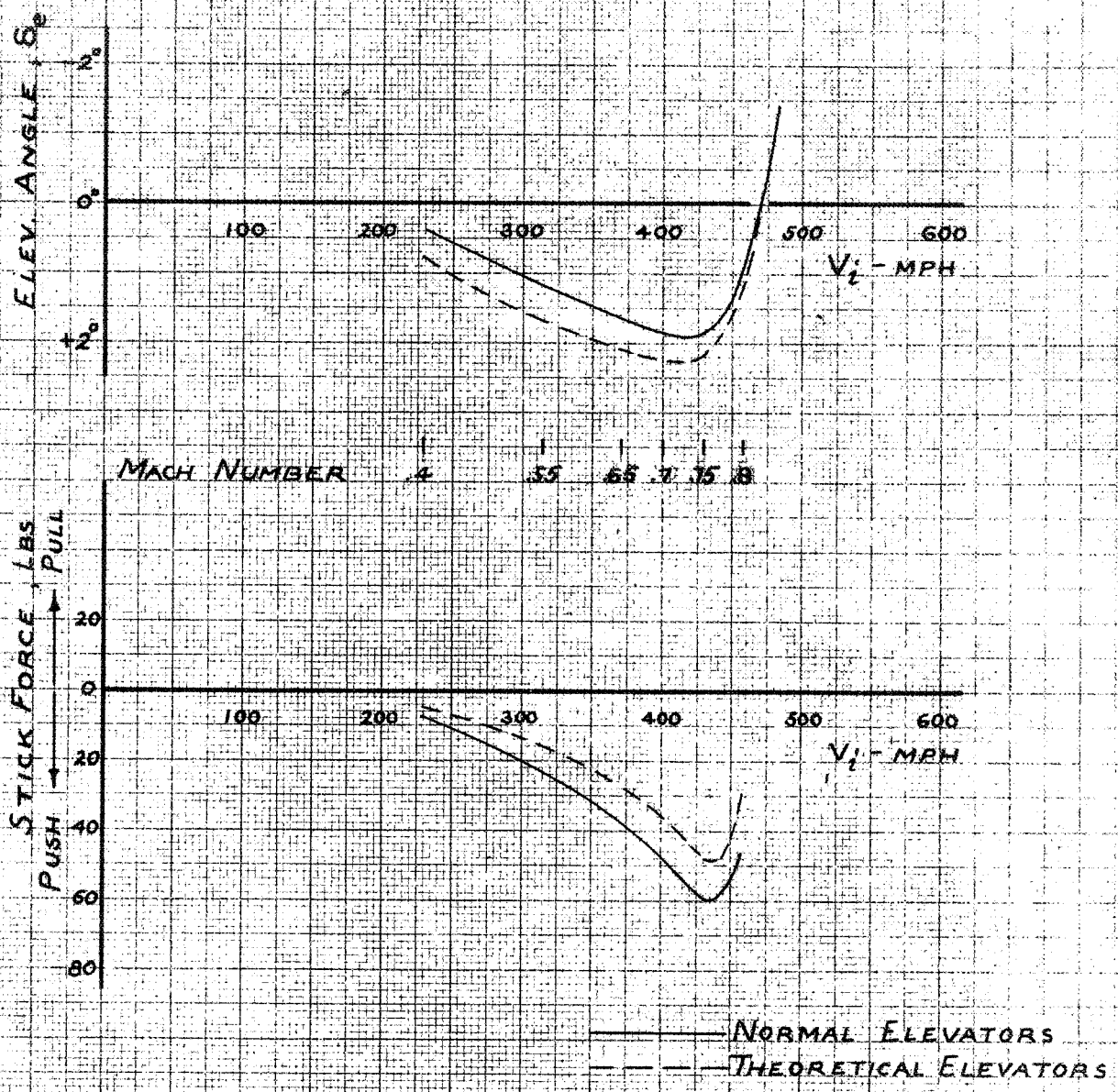

(b) h = 15000 FEET

FIGURE 13.- CONTINUED. P-39N-1 MODEL.

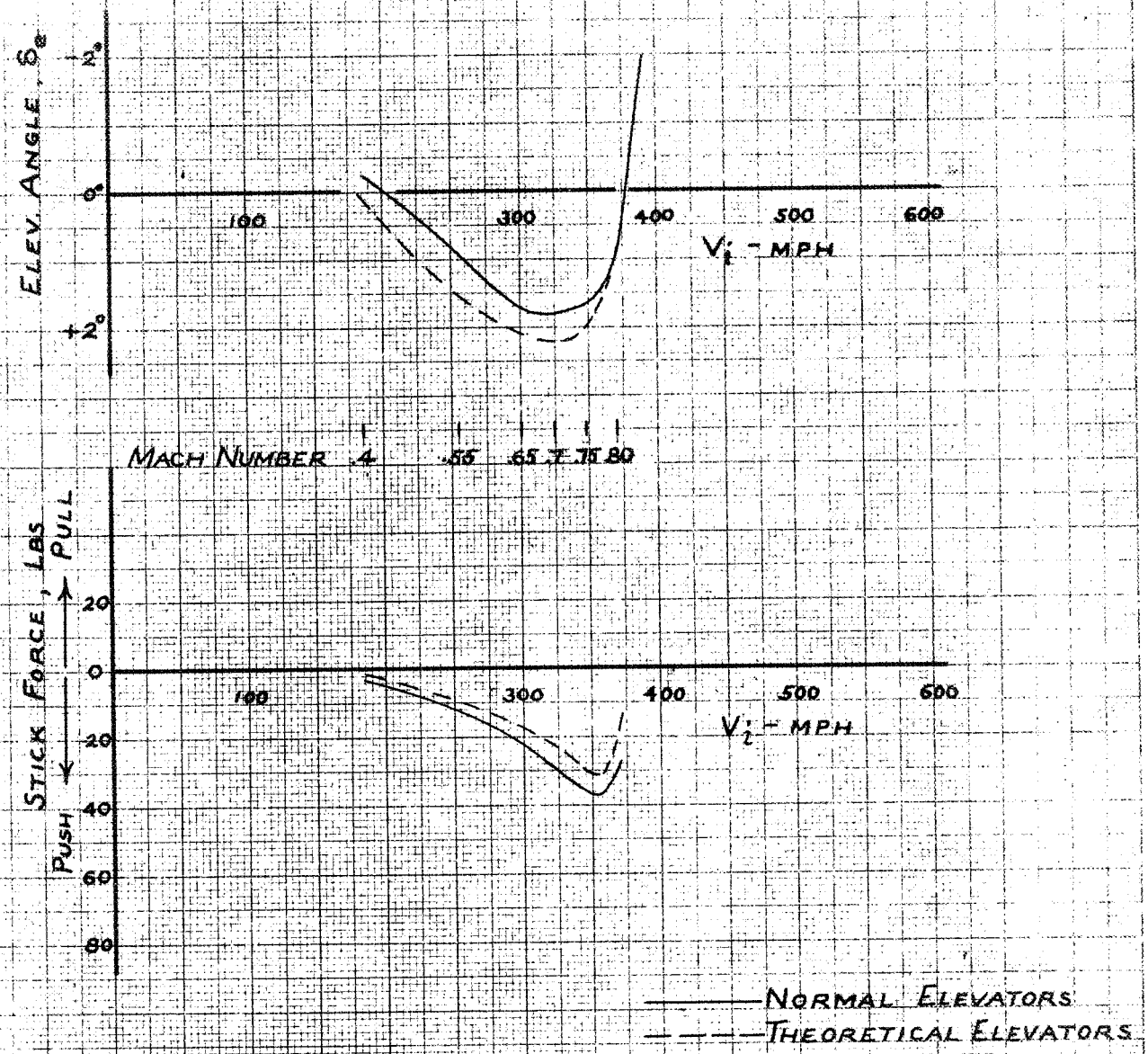

(c) $h = 25000$ FEET.

FIGURE 13.- CONCLUDED P-39N-1 MODEL

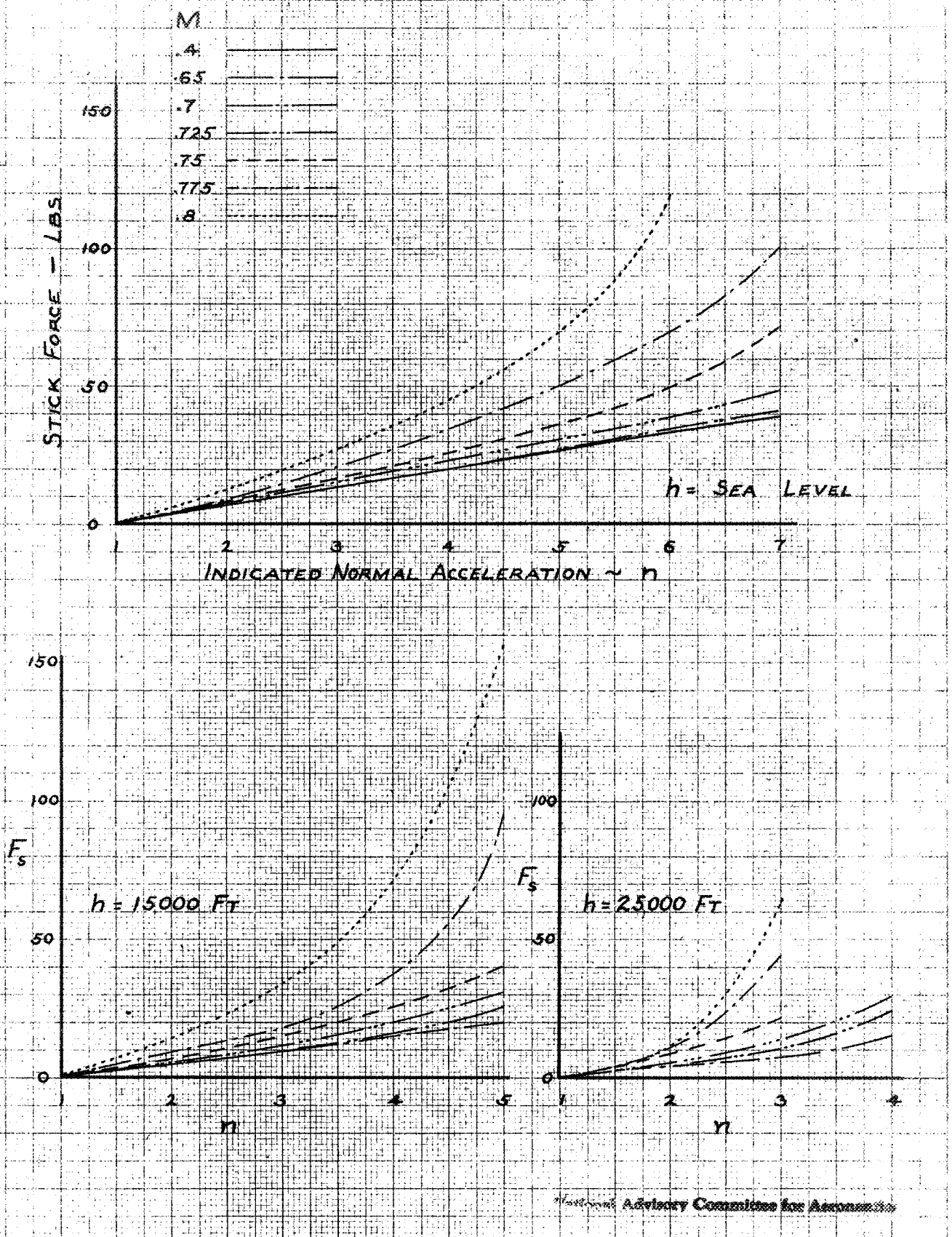

FIGURE 14.— VARIATION OF STICK FORCE WITH INDICATED NORMAL ACCELERATION FOR VARIOUS MACH NUMBERS AT DIFFERENT ALTITUDES. NORMAL ELEVATORS; $i_t = 2\frac{1}{4}°$

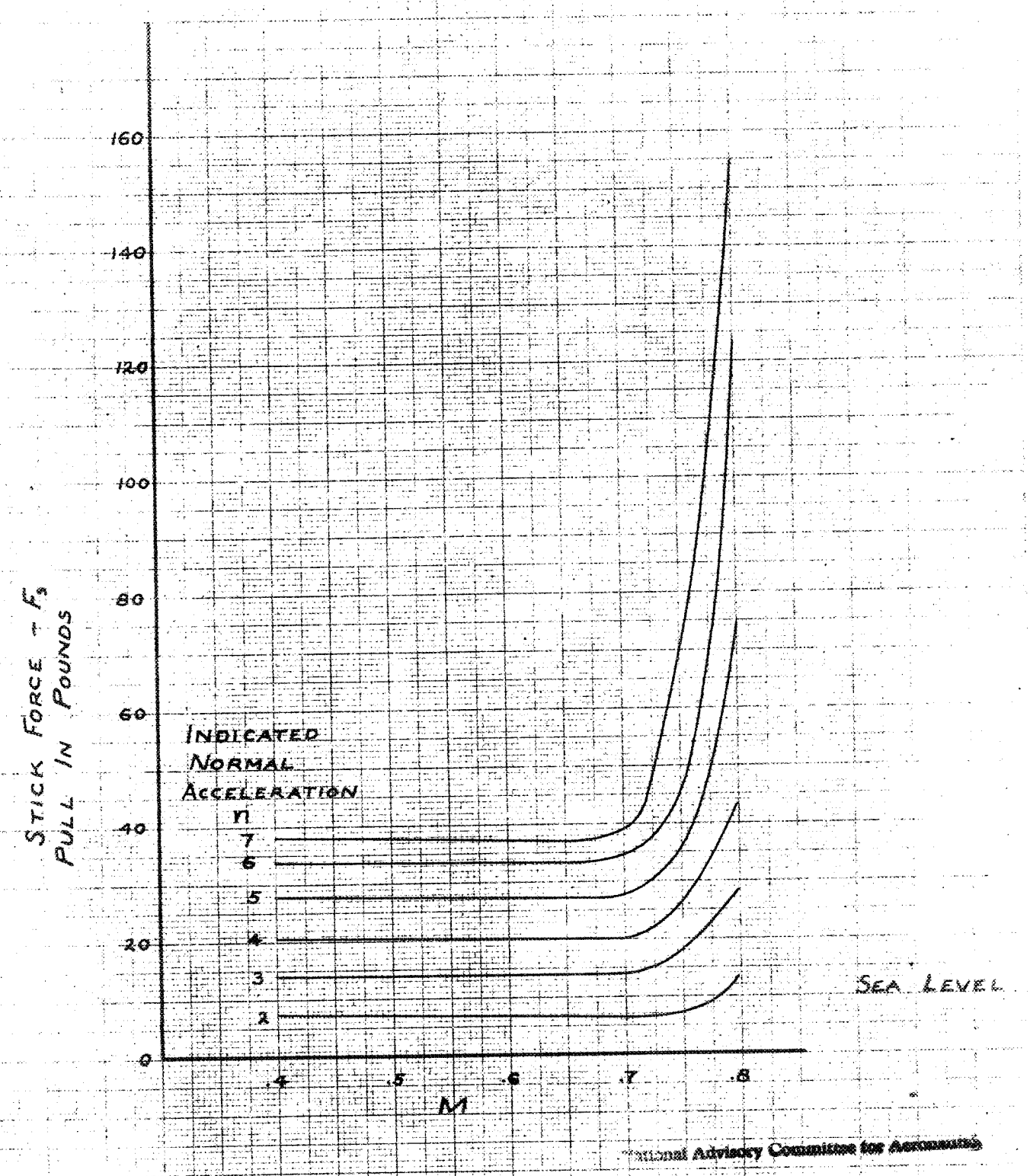

FIGURE 15.— VARIATION OF STICK FORCE WITH MACH NUMBER FOR CONSTANT VALUES OF INDICATED NORMAL ACCELERATION. NORMAL ELEVATORS; $i_t = 2\frac{1}{4}°$; P-39N-1 MODEL.